Geoderma 462 (2025) 117523

Contents lists available at ScienceDirect

Geoderma

journal homepage: www.elsevier.com/locate/geoderma

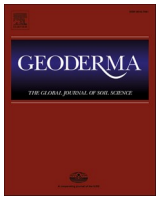

Temporal-spatial characteristics and environmental controls of annual CH_4 fluxes in a Tibetan alpine landscape

Zhisheng Yao [a,b,c,*], Rui Wang [a], Han Zhang [a], Lei Ma [a], Xunhua Zheng [a,b], Kai Wang [a], Wei Zhang [a], Yong Li [a,b], Bo Zhu [d], Klaus Butterbach-Bahl [a,c,e]

[a] State Key Laboratory of Atmospheric Environment and Extreme Meteorology, Institute of Atmospheric Physics, Chinese Academy of Sciences, Beijing 100029, PR China
[b] College of Earth and Planetary Science, University of Chinese Academy of Sciences, Beijing 100049, PR China
[c] Pioneer center Land-CRAFT, Department of Agroecology, Aarhus University, 8000 Aarhus C, Denmark
[d] Key Laboratory of Mountain Surface Processes and Ecological Regulation, Institute of Mountain Hazards and Environment, Chinese Academy of Sciences, Chengdu 610041, PR China
[e] Institute for Meteorology and Climate Research, Atmospheric Environmental Research, Karlsruhe Institute of Technology, Garmisch-Partenkirchen 82467, Germany

ARTICLE INFO

Handling Editor: Dr Daniel Said-Pullicino

Keywords:
Methane
Meadow
Wetland
Soil moisture
Non-growing season
Alpine ecosystem
Tibetan Plateau

ABSTRACT

Alpine ecosystems on the Tibetan Plateau are characterized by different soil hydrothermal conditions and vegetation composition across the elevation gradient, and contribute differently to the net landscape methane (CH_4) budget. However, the spatiotemporal variation of CH_4 fluxes from alpine ecosystems remains poorly understood, underpinning the uncertainty of upscaling the regional and global CH_4 budgets. Here, we investigated the spatial and temporal patterns and environmental controls of CH_4 fluxes over two years across a Tibetan alpine landscape spanning different elevations (spanning 3200–3500 m above sea level) and major ecosystem types (including alpine meadow, steppe, forest and wetland). On the annual scale, all alpine upland (meadow, steppe and forest) ecosystems consistently functioned as soil CH_4 sinks, ranging between 1.12 and 2.49 kg C ha^{-1} yr^{-1}, whereas alpine wetlands emitted 17.2–34.3 kg C ha^{-1} yr^{-1} to the atmosphere. Non-growing season CH_4 fluxes accounted for 29–46 % of the annual budgets, underscoring its significant contribution that was often neglected in previous studies. Our study also demonstrated that for individual alpine upland and wetland ecosystems, soil water content and soil temperature were the main factors regulating the seasonal patterns of CH_4 fluxes. While across all alpine ecosystems, soil water content outweighed temperature as the primary control on the landscape patterns of CH_4 fluxes and higher wetland CH_4 emissions were associated with increased soil inorganic N availability. Despite their small area contribution to the landscape, alpine wetlands emitted disproportionate amounts of CH_4, weakening the landscape CH_4 sink. The resulting net landscape CH_4 balance was a weak sink of 0.72 kg C ha^{-1} yr^{-1}. Overall, the multiple parameters and insights gained from our study provide valuable information for better predicting the role of alpine ecosystem CH_4 carbon-climate feedbacks in high-altitude regions.

1. Introduction

Methane (CH_4) is the second most potent greenhouse gas (GHG) after carbon dioxide (CO_2), contributing to a radiative forcing of 0.54 W/m^2 or about one-third of global warming (IPCC, 2021; Jiang et al., 2024). Recent monitoring indicates that the globally averaged atmospheric concentration of CH_4 has nearly tripled since pre-industrial times (WMO, 2019). This rapid increase in atmospheric CH_4 concentrations has been attributed to a shift in the balance between its sources and sinks (Zhou et al., 2024). Although powerful, CH_4 is a short-lived climate forcer with an atmospheric lifetime of ca. 9 years. This means that reductions in CH_4 emissions can yield immediate benefits by decreasing atmospheric concentrations and thus mitigating near-term warming (Jiang et al., 2024). Therefore, achieving the 1.5 °C goal of the Paris Agreement requires balancing sources and sinks of CH_4, particularly to reverse the rise in atmospheric CH_4 concentrations (Nisbet, 2023; Fu et al., 2024). Moreover, emissions of CH_4 contribute to the effective formation of tropospheric ozone (O_3), which causes nearly half a million premature deaths each year and threatens ecosystem productivity (Shindell et al., 2012; Feng et al., 2022). Recognizing the direct and

* Corresponding author.
E-mail address: zhishengyao@mail.iap.ac.cn (Z. Yao).

https://doi.org/10.1016/j.geoderma.2025.117523
Received 23 June 2025; Received in revised form 1 September 2025; Accepted 24 September 2025
Available online 28 September 2025

indirect leverage of CH_4 in mitigating climate change, improving public health and alleviating food shortages, more than 100 countries launched the Global Methane Pledge initiative at the 2021 United Nations Climate Change Conference (COP26) to reduce CH_4 emissions by at least 30 % by 2030 (https://www.globalmethanepledge.org/). However, due to a lack of reliable estimates of the various sources and sinks of atmospheric CH_4, there are still significant uncertainties in the current global CH_4 budget.

One source of uncertainty for the global CH_4 budget is the relative importance of soils as sources and sinks of atmospheric CH_4, as net CH_4 exchange at the soil-atmosphere interface can be highly variable in space and time. It has been estimated that soils as a global CH_4 sink can remove 11–49 Tg CH_4 yr^{-1} from the atmosphere (Saunosi et al., 2020). The range of estimates for CH_4 emissions from soils, such as in natural wetlands is also large, ranging from 92 to 281 Tg CH_4 yr^{-1} (Song et al., 2015; Peng et al., 2019). CH_4 consumption occurs mainly in aerated upland soils by methanotrophic bacteria, which oxidize CH_4 to CO_2 (Conrad, 1996). Conversely, CH_4 production (methanogenesis) occurs in saturated or wetland soils through the microbial reduction of acetate or hydrogen (H_2) and CO_2, but simultaneously anaerobic oxidation of CH_4 (AOM) can also occur (Conrad, 1996; Gauthier et al., 2015). Hence, methanotrophic and methanogenic activities and the net CH_4 fluxes are often regulated by a number of abiotic and biotic factors (such as soil temperature, moisture, substrate availability, pH, oxygen status and plant phenology and production) within the soil profile and at different spatial and temporal scales (West et al., 1999; Olefeldt et al., 2013; D'Imperio et al., 2017; Kaiser et al., 2018; Yu et al., 2019). Furthermore, the key factors or parameters controlling CH_4 fluxes are often different and difficult to determine across ecosystems, which further complicates regional and global CH_4 budgeting analyses (Luo et al., 2013; Bridgham et al., 2013; Kaiser et al., 2018). However, a number of studies have demonstrated that landscape-level analyses are useful for assessing the spatial heterogeneity of soil hydrological processes and biogeochemical carbon (C) and nitrogen (N) cycles (Creed et al., 2002; Riveros-Iregui and McGlynn, 2009; Duncan et al., 2013; Anderson et al., 2015; Wangari et al., 2023), which are closely related to the magnitude and variability of CH_4 fluxes. To reduce uncertainties in estimating soil CH_4 sources or sinks, therefore, it is critical to better understand the spatiotemporal patterns and environmental controls of CH_4 fluxes at the landscape scale.

Soils in high-latitude and high-altitude regions contain more than half of the world's soil organic C (Hugelius et al., 2014; Yang et al., 2023), and play an important role in the global C cycle and associated CH_4 fluxes. Among them, the Tibetan Plateau (also called Third Pole of the World) is the largest high-altitude region in the world (Chen et al., 2024). Due to the high spatial heterogeneity of the plateau, such as differences in temperature, precipitation and nutrient supply along the elevation gradient, the land areas of the Tibetan Plateau are characterized by different soil and vegetation types such as alpine forests, grasslands (including meadows and steppes) and wetlands, which are the dominant landscape elements in this region (Yao et al., 2022; Chen et al., 2022). Hence, whether soils act as a net source or sink of CH_4 across the Tibetan alpine landscape depends on the relative contribution of these land cover/ecosystem types to the net CH_4 budget. In recent decades, a growing number of studies have been conducted in different Tibetan alpine ecosystems, and they have shown that alpine grasslands act as net CH_4 sinks (e.g., Jiang et al., 2010; Wei et al., 2015; Zhu et al., 2015; Fu et al., 2018) while alpine wetlands functioned as net CH_4 sources (Hirota et al., 2005; Chen et al., 2008; Yu et al., 2013; Song et al., 2015; Peng et al., 2019). For these individual ecosystems, the temporal dynamics of CH_4 fluxes are expected to depend on their specific soil hydrothermal conditions. For example, Song et al. (2015) found a significant relationship between CH_4 emissions and soil temperature and water table depth in a Tibetan alpine wetland. Wei et al. (2015) reported that CH_4 uptake during the growing season was well correlated with soil moisture/temperature for alpine steppe and meadow. Nevertheless, although decadal efforts have been made, most of them have focused on assessing CH_4 fluxes from one or two ecosystem types. This limits the investigation of landscape patterns (with different ecosystem types) and their controlling factors of CH_4 fluxes. Besides, due to the extremely harsh environment, especially during winter months on the Tibetan Plateau, most previous studies either focused only on growing season CH_4 fluxes or were conducted with coarse sampling frequency (monthly or seasonally) for the non-growing season (e.g., Jiang et al., 2010; Kato et al., 2011; Wei et al., 2015; Li et al., 2015). Given that non-growing season CH_4 fluxes are likely to be an important component and may even dominate the annual budgets in cold climate regions (e.g., Mastepanov et al., 2008; Chen et al., 2011; Song et al., 2015; Treat et al., 2018), it is critical to investigate the sign and magnitude of CH_4 fluxes from different Tibetan alpine landscape elements on annual time scales.

Here, we report the results of a 2-year field study in which annual CH_4 fluxes and their association with environmental variables (e.g., soil temperature, moisture and C and N substrate availability) were observed from a larger number of sites across the alpine landscape encompassing different altitudes and ecosystem types (including alpine forest, meadow, steppe and wetland) on the Tibetan Plateau. Therefore, the objectives of this study were accordingly (1) to assess the temporal and spatial characteristics of CH_4 fluxes across the Tibetan alpine landscape; (2) to examine how these environmental factors relate to CH_4 fluxes; and (3) to estimate net landscape-scale CH_4 balances. We hypothesized that due to the expected large variability of CH_4 fluxes between upland ecosystems functioning as net CH_4 sinks and wetland ecosystems functioning as net CH_4 sources, and despite the relatively small area of wetland systems, alpine wetlands significantly affect the CH_4 budget at the landscape scale.

2. Materials and methods

2.1. Study sites

The study was carried out within a Zoige catchment (34°01′–34°03′N, 102°43′–102°44′E, 3200–3500 m a.s.l. (above sea level)) on the eastern Tibetan Plateau of China. The area experiences a cool humid continental monsoon climate characterized by long cold winters and short cool summers. Based on long-term meteorological data (1980–2012), the mean annual air temperature is 1.6 ± 0.6 °C (mean ± standard deviation), with the warmest monthly mean of 11.2 ± 0.9 °C during July and the coldest monthly mean of −9.6 ± 1.6 °C during January. The mean annual precipitation is 649 ± 94 mm, of which about 85 % occurs during the growing season from mid-April to October (Yao et al., 2022).

The catchment is characterized by a typical and representative alpine landscape, with geomorphological, hydrological, vegetative and climatological heterogeneity across the elevation gradient (Zhang et al., 2022). The landscape covers an area of about 189 ha, excluding the human infrastructure areas such as settlements and roads. The main land cover/ecosystem types within the landscape are alpine meadow, forest, wetland and steppe along the gradient from 3200 to 3500 m a.s.l.. The alpine meadow totally covers about 123 ha (65.2 %) and are mainly distributed at three altitudes, i.e., at the elevation of 3430 m (referred to as M3430), 3326 m (referred to as M3326) and 3231 m (referred to as M3231). The forest covers about 44 ha (23.1 %) and is mainly located at the elevation of 3415 m (referred to as F3415). The wetland covers only about 9 ha (4.6 %) and is located at an elevation of 3304 m (referred to as W3304). The steppe covers about 14 ha (7.1 %) and is located at an elevation of 3245 m (referred to as S3245). Twenty-eight sampling sites or plots (approximately 20 × 25 m each) were established at six different elevational landscape elements, including M3430 (n = 4 sites), F3415 (n = 6 sites), M3326 (n = 4 sites), W3304 (n = 6 sites), S3245 (n = 4 sites) and M3231 (n = 4 sites). Note that site W3304 is a seasonally flooded (usually in summer) alpine wetland, characterized by a unique micro-topography with numerous scattered hummocks, hollow water-

holes, and transition areas between hummocks and hollow water-holes. To represent the complex characteristics, we randomly established three plots each within the W3304 site: the hummock (referred to as W3304-H), hollow water (referred to as W3304-W) and transition (referred to as W3304-T) micro-topographies, resulting in a total of 18 plots for the alpine wetland. For more details on the design of the different elevational sites, see Yao et al. (2022). According to the local management regime, all alpine ecosystems except for F3415 within the landscape were used for grazing with Tibetan sheep and yak during the winter and late spring to early summer. Stocking rates ranged from 0.47 to 3.49 sheep unit ha^{-1} yr^{-1}. Further information on site characteristics such as coordinates, dominant vegetation species and soil physicochemical properties are presented in Table S1.

2.2. Methane flux measurements

CH_4 fluxes at all study sites were measured from November 2013 to October 2015, using an opaque static chamber-based technique (Zhang et al., 2019). Specifically, field sampling was performed over a year-long campaign for sites M3430, F3415 and S3245, and over a two-year period for sites M3326, W3304 and M3231 (Table S1). In general, soil CH_4 fluxes were measured two or three times per week with an interval of 2–3 days during the growing season. During the non-growing season, they were measured once per week. For the flux measurements, a square stainless-steel frame (0.5 m × 0.5 m) was permanently inserted into the soil at a depth of 10 or 15 cm in the center of each spatially replicated site or plot. To eliminate the possibility of the temporary installation of chamber bases influencing CH_4 fluxes, the frames were set up at least two weeks before the initial measurements and maintained in place throughout the entire observation period. A total of 40 base frames were installed in the different elevation ecosystems, i.e., 4 for M3430, 6 for F3415, 4 for M3326, 6 for W3304-H, 6 for W3304-T, 6 for W3304-W, 4 for S3245 and 4 for M3231. On each sampling day (usually between 09:00 am and 11:00 am), the vented, insulated stainless-steel chambers (0.5 m × 0.5 m with a height of 0.15 or 0.5 m, depending on plant growth) were mounted on the base frames, and five gas samples were collected using 60 mL polypropylene syringes at 10-min intervals after the chamber closure (i.e., at time 0, 10, 20, 30 and 40 min, respectively). Gas samples were analyzed for CH_4 at an on-site laboratory within 6 h of sampling, using an Agilent 7890A gas chromatography system (GC, Agilent Technologies, Santa Clara, CA, USA) outfitted with a flame ionization detector (FID) at 200 ℃. A certified standard gas (containing 2.15 ppmv CH_4) was used for instrument calibration. The repeatability of the CH_4 standard was better than 1 %. CH_4 fluxes were calculated by linear or nonlinear fitting of changes in chamber headspace CH_4 concentrations over 40 min (Hutchinson and Livingston, 1993). The details of these chamber-based measurements are described in previous works (Zhang et al., 2019; Yao et al., 2025). The minimum detection limit of the CH_4 flux was about ± 1.4 μg C m^{-2} h^{-1} for the methods and procedures used.

2.3. Auxiliary data

Meteorological parameters including daily precipitation, barometric pressure and air temperature were measured by an automated weather station located at the M3326 site. Soil temperature, soil moisture, and soil ammonium (NH_4^+), nitrate (NO_3^-) and dissolved organic carbon (DOC) concentrations were as well measured during the study period. Soil temperature at 5 cm depth was recorded every 30 min using HOBO temperature sensors (Hobo Data Logger UTBI-001, Onset, USA). Soil moisture at 0–6 cm depth was monitored as volumetric water content using a portable frequency domain reflectometry probe (MPM-160, Jiangsu RDS Technology Co. Ltd., China). When the soil was frozen during the winter time, soil moisture was determined gravimetrically on soil samples taken from each site or plot. Here soil water content for all study sites is reported as water-filled pore space (WFPS), which was calculated using the volumetric or gravimetric water content and bulk density for the upland ecosystem sites (i.e., M3430, F3415, M3326, S3245 and M3231) (Yao et al., 2024) and using the measured volumetric water content and total porosity for the W3304 sites (Zhang et al., 2019). The NH_4^+, NO_3^- and DOC concentrations at 0–10 cm soil depth were determined at 1–2 weeks intervals by collecting three replicated soil samples from each site or plot. After extraction of soil samples with 1 M KCl solution (for NH_4^+ and NO_3^-) and deionized water (for DOC), respectively, in a soil:solution ratio of 1:5, soil NH_4^+, NO_3^- and DOC contents were measured using a colorimetric Flow Injection Analyzer (San + +, Skalar Analytical B.V., Netherlands). In addition, the perforated polyvinyl chloride pipes were inserted into the soil to a depth of 4.0 m at the W3304 sites, and water table depths (WTD) were measured with a ruler from May 2014 to October 2015. Negative values for WTD represent water table depths below the soil surface.

2.4. Data and statistical analyses

Seasonal and annual cumulative CH_4 uptake rates or emissions for all sites were estimated by linear interpolation between sampling dates over the given period (e.g., the growing season, non-growing season and annual scale). Daily, seasonal and annual CH_4 emissions for W3304 were reported as the area-weighted means of those from each type of micro-topography (i.e., W3304-H, W3304-T and W3304-W). Based on the areal contributions of the different elevation ecosystems within the alpine landscape, we estimated the landscape-scale CH_4 balances (or the so-called area-weighted CH_4 fluxes for the whole landscape). Analysis of variance (ANOVA) or non-parametric tests were used to assess the significance of differences in cumulative CH_4 uptake rates or emissions between the different elevation sites. Linear, nonlinear or multiple regression analysis was used to understand the significant relationships between CH_4 uptake rates or emissions and environmental variables. The best regression model was selected based on the coefficient of determination (R^2) and the Akaike Information Criterion (AIC). We performed a Random Forest (RF) analysis using the R package "randomForest" to determine the relative importance of individual environmental factors on the temporal variability of CH_4 fluxes. Additionally, we used the "glmulti" R package for model selection analysis to identify the important predictors of the spatial characteristics of annual CH_4 fluxes. We expressed the relative importance of each predictor as the sum of Akaike weights for all potential models that included the predictor, and a cutoff of 0.8 was set to differentiate between important and nonessential predictors (Terrer et al., 2016). A temperature sensitivity coefficient (Q_{10}) was calculated based on the Arrhenius equation by plotting CH_4 uptake rates or emissions against soil temperature (Yao et al., 2010). All statistical analyses were conducted using SPSS 19.0 for Windows (SPSS China, Beijing, China), and statistical significance was accepted by values of $P < 0.05$ unless otherwise stated.

3. Results

3.1. Environmental variables

Relative to the long-term mean annual temperature of 1.6 °C, both study years appear to be warmer with mean values of 2.7 and 3.1 °C for 2013–2014 and 2014–2015, respectively (Fig. S1). Compared to the long-term average rainfall of 649 mm, the annual precipitation is comparable in the 2013–2014 year (615 mm) while it appears to be drier in the 2014–2015 year (458 mm). Soil temperatures at all sites showed a similar seasonal pattern, characterized by significantly higher values during the growing season compared to the non-growing season (Figs. 1 and 2). Annual mean soil temperatures for alpine upland sites (M3430, F3415, M3326, S3245 and M3231) ranged from 3.2 to 8.4 °C, decreasing significantly with increasing elevation (Table 1). For alpine wetland sites, the mean soil temperatures ranged from 4.6 to 5.5 °C, with no

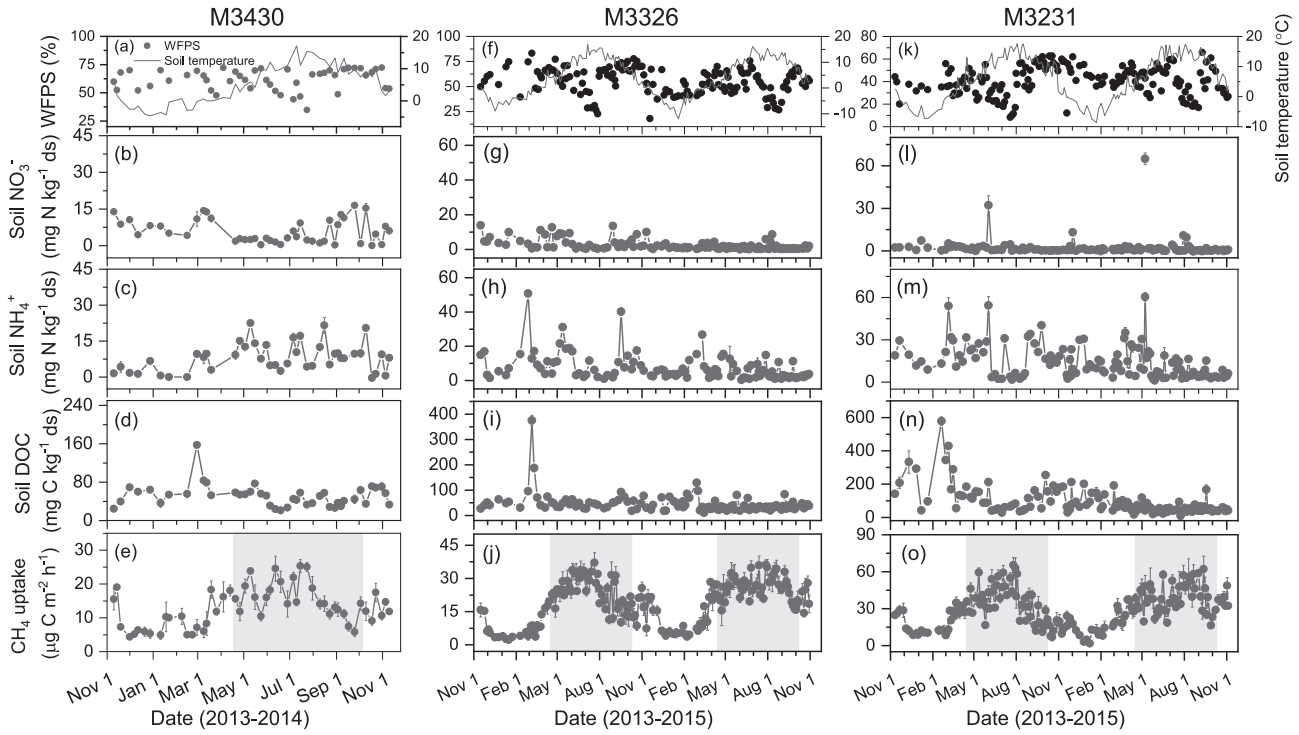

Fig. 1. Seasonal patterns of (a, f and k) soil temperature and water-filled pore space (WFPS), (b, g and l) soil nitrate (NO_3^-), (c, h and m) ammonium (NH_4^+) and (d, i and n) dissolved organic carbon (DOC) concentrations and (e, j and o) methane (CH_4) uptake rates from alpine meadows at elevations of 3430 (M3430), 3326 (M3326) and 3231 m (M3231), respectively, over the study period 2013–2015. The vertical bars indicate standard errors of 4 spatial replicates. The gray shaded area indicates the vegetation-growing season.

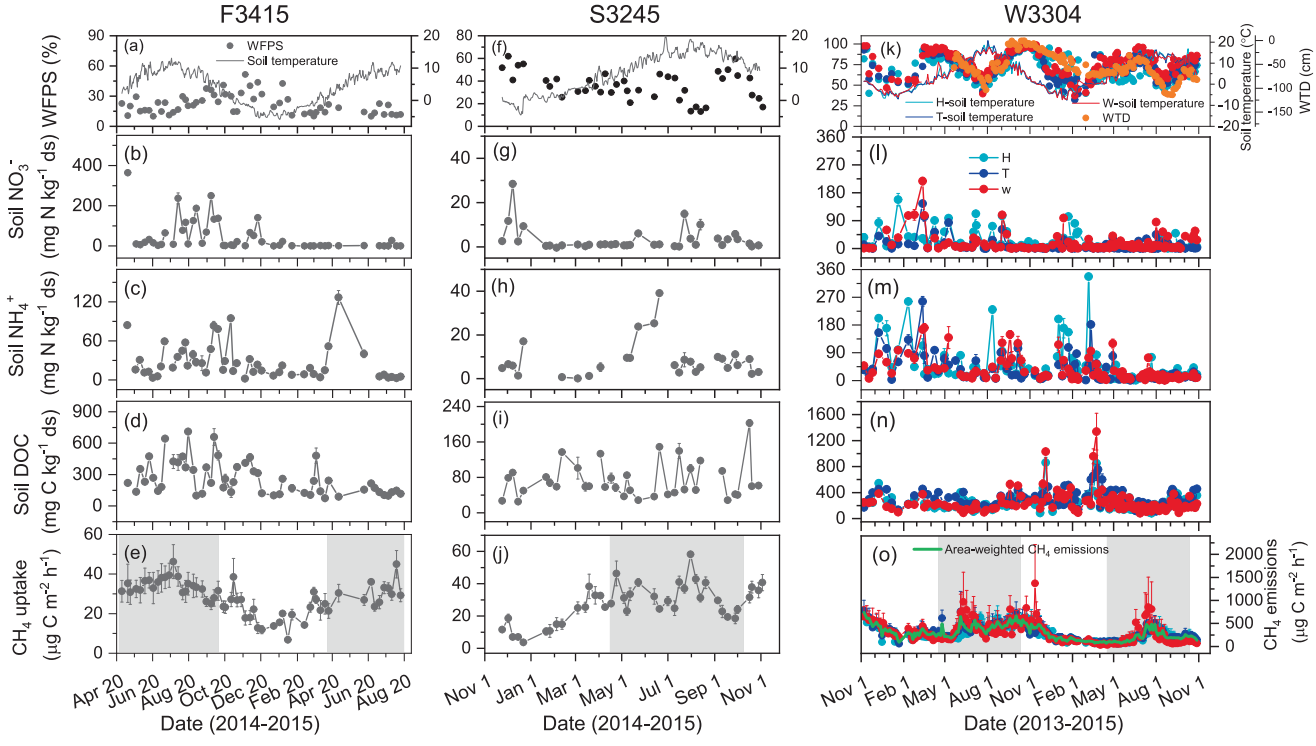

Fig. 2. Seasonal patterns of (a, f and k) soil temperature, water-filled pore space (WFPS) and water table depth (WTD), (b, g and l) soil nitrate (NO_3^-), (c, h and m) ammonium (NH_4^+) and (d, i and n) dissolved organic carbon (DOC) concentrations and (e and j) methane (CH_4) uptake rates or (o) emissions from alpine forest at the elevation of 3415 m (F3430), steppe at the elevation of 3245 m (S3245) and wetland at the elevation of 3304 m (W3304), respectively, over the study period 2013–2015. Micro-topographies of wetlands: −H = hummocks, −T = transition between micro-topographies, −W = hollow water holes. The vertical bars indicate standard errors of 4–6 spatial replicates. Negative values of WTD = below ground. Area-weighted CH_4 emissions in panel (o) are calculated in terms of the areal extent of 20 %, 71 % and 9 % for the W3304-H, W3304-T and W3304-W, respectively. The gray shaded area indicates the vegetation-growing season. The legend in panel (l) also applies for other panels of W3304.

Table 1
Mean soil temperature, water-filled pore space (WFPS) and concentrations of ammonium (NH_4^+), nitrate (NO_3^-) and dissolved organic carbon (DOC) across the annual scale and annual cumulative methane (CH_4) uptake or emission for different ecosystem sites along the elevation gradient in a Tibetan alpine landscape over the period 2013–2015.

Year	Ecosystem type	Soil temperature (°C)	WFPS (%)	NH_4^+ (mg N kg^{-1}ds)	NO_3^- (mg N kg^{-1}ds)	DOC (mg C kg^{-1}ds)	Annual CH_4 uptake or emission (kg C ha^{-1} yr^{-1})
Upland sites							
2013–2014	M3430	4.6 ± 0.8b	58.3 ± 11.8 a	7.9 ± 0.9b	6.5 ± 0.8 a	51.8 ± 3.4b	1.12 ± 0.08b
	M3326	5.4 ± 0.7 ab	60.3 ± 13.0 a	11.0 ± 1.6b	4.5 ± 0.6 a	58.8 ± 8.4b	1.42 ± 0.05b
	M3231	6.8 ± 0.8 a	40.2 ± 13.9 a	18.0 ± 1.8 a	1.6 ± 0.2b	148 ± 16.8 a	2.33 ± 0.09 a
2014–2015	F3415	3.2 ± 0.7b	20.2 ± 11.1c	27.4 ± 3.9 a	46.1 ± 11.2 a	339 ± 49.2 a	2.26 ± 0.11 a
	M3326	4.9 ± 0.8b	53.6 ± 13.5 a	5.0 ± 0.6c	1.3 ± 0.2c	37.7 ± 2.3c	1.63 ± 0.05b
	S3245	8.4 ± 0.9 a	36.1 ± 1.5b	8.6 ± 0.6b	3.4 ± 0.4b	73.0 ± 5.2b	2.21 ± 0.11 a
	M3231	6.8 ± 0.8 a	41.7 ± 11.9 bc	10.4 ± 0.9b	1.3 ± 0.2c	64.8 ± 4.3b	2.49 ± 0.04 a
Wetland sites							
2013–2014	W3304-H	5.5 ± 0.8 a	73.8 ± 14.9 a	60.6 ± 9.9 a	36.3 ± 6.3 a	247 ± 14.5 a	29.9 ± 9.7 a
	W3304-T	5.3 ± 0.8 a	77.3 ± 14.7 a	53.6 ± 8.5 a	20.1 ± 5.4 a	294 ± 14.5 a	33.6 ± 9.6 a
	W3304-W	5.4 ± 0.7 a	81.0 ± 14.7 a	57.7 ± 8.0 a	28.7 ± 7.8 a	221 ± 16.1 a	34.3 ± 11.8 a
	W3304					*Area-weighted emission*: 32.9 ± 9.8	
2014–2015	W3304-H	5.3 ± 0.7 a	65.8 ± 12.5 a	35.7 ± 6.5 a	12.0 ± 2.1 a	257 ± 15.3 a	17.2 ± 6.0 a
	W3304-T	4.9 ± 0.7 a	67.9 ± 13.6 a	21.1 ± 3.7 a	6.2 ± 1.1b	302 ± 16.0 a	17.3 ± 5.4 a
	W3304-W	4.6 ± 0.7 a	74.3 ± 13.4 a	22.0 ± 3.3 a	13.8 ± 2.2 a	263 ± 22.7 a	17.4 ± 7.0 a
	W3304					*Area-weighted emission*: 17.3 ± 5.7	

Values represent mean ± standard error (n = 4–6). ds, dry soil. Ecosystem types are coded as follows: M = alpine meadow; F = alpine forest; S = alpine steppe; W = alpine wetland; 6-digit numbers = elevation in m above sea level; micro-topographies of wetlands: −H = hummocks, −T = transition between micro-topographies, −W = hollow water holes. Area-weighted CH_4 emission was calculated in terms of the areal extent of 20 %, 71 % and 9 % for the W3304-H, W3304-T and W3304-W, respectively. Different letters within the same column indicate significant differences among the ecosystems in each year at the $P < 0.05$ level.

significant differences among the W3304-H, W3304-T and W3304-W sites. Soil WFPS for all upland sites varied between 10 % and 80 %, with annual means of 58 %, 20 %, 57 %, 36 % and 41 % for M3430, F3415, M3326, S3245 and M3231, respectively. The WFPS for alpine grassland sites (including M3430, M3326, S3245 and M3231) increased significantly with increasing altitude. Compared to the upland sites, the W3304 sites showed significantly higher WFPS (range: 40–99 %; mean: 66–81 %) (Table 1). Similarly, the W3304 sites had relatively higher soil NH_4^+ and NO_3^- as well as DOC concentrations, compared to all upland sites except the alpine forest (Table 1). In addition, the WTD at the W3304 sites was usually below the soil surface, ranging from −114 to −1 cm (Fig. 2k).

3.2. Temporal variations of CH_4 uptake rates or emissions

During the study period, all alpine upland sites functioned exclusively as net sinks for atmospheric CH_4 (Figs. 1 and 2). The CH_4 uptake at the upland sites showed clear and similar seasonal patterns, characterized by significant uptake rates during the growing season and lower values during the non-growing season. The CH_4 uptake rates varied from 4.4-25.3 μg C m^{-2} h^{-1} for M3430, 6.8–46.3 μg C m^{-2} h^{-1} for F3415, 2.2–38.0 μg C m^{-2} h^{-1} for M3326, 3.7–58.2 μg C m^{-2} h^{-1} for S3245 and 1.7–65.3 μg C m^{-2} h^{-1} for M3231. Across individual observations, there was a significant exponential relationship between CH_4 uptake rates and soil temperature at each upland site, and approximately 37–64 % of the variation in CH_4 uptake rates could be explained by the changes in soil temperature (Fig. 3). The resulting Q_{10} values ranged from 1.51 to 1.90 for all alpine upland sites (Table S2). In addition to soil temperature, the variance of CH_4 uptake rates at each upland site was also affected by soil WFPS, and they had a significant negative relationship (Fig. 4). Moreover, the sensitivity of CH_4 uptake rates to soil temperature or WFPS was further investigated by synthesizing the dataset across all upland sites. The analysis results showed that CH_4 uptake rates were positively correlated with soil temperature, but negatively correlated with WFPS (Fig. 5). We also included soil temperature and WFPS in multiple regression analysis to examine their combined effects. As shown in Fig. 6 and Table S3, up to 63–78 % of the variation in CH_4 uptake rates could be explained by the combined effects of soil temperature and WFPS. Moreover, RF model analysis confirmed that soil temperature and WFPS were the key factors influencing the temporal variability of CH_4 uptake at upland sites, with the relative importance exceeding 70 % (Fig. S2).

In contrast to the upland sites, alpine wetlands functioned as net sources of atmospheric CH_4 throughout the study period (Fig. 2). Generally, the growing season exhibited relatively higher CH_4 emissions compared to the non-growing season. The CH_4 emissions ranged from 54-644 μg C m^{-2} h^{-1}, 59–779 μg C m^{-2} h^{-1} and 33–1371 μg C m^{-2} h^{-1} for sites W3304-H, W3304-T and W3304-W, respectively, with their area-weighted emissions ranging from 71 to 740 μg C $m^{-2}h^{-1}$. Regression analysis showed that the changes in both soil temperature and WFPS had very strong positive effects on the variance of CH_4 emissions at the W3304 sites (Figs. 3 and 4). An exponential function can be used to describe the soil temperature dependence of CH_4 emissions, and the resulting Q_{10} value was 1.23 (Table S2). The combined effects of soil temperature and WFPS could explain about 37 % of the observed variation in CH_4 emissions (Fig. 6 and Table S3). In addition, there was a significant exponential relationship between CH_4 emissions and WTD (Fig. 5). RF model analysis also showed that soil temperature, WTD and WFPS were the main drivers in shaping the temporal variability of wetland CH_4 emissions, with scaled importance measures ranging from

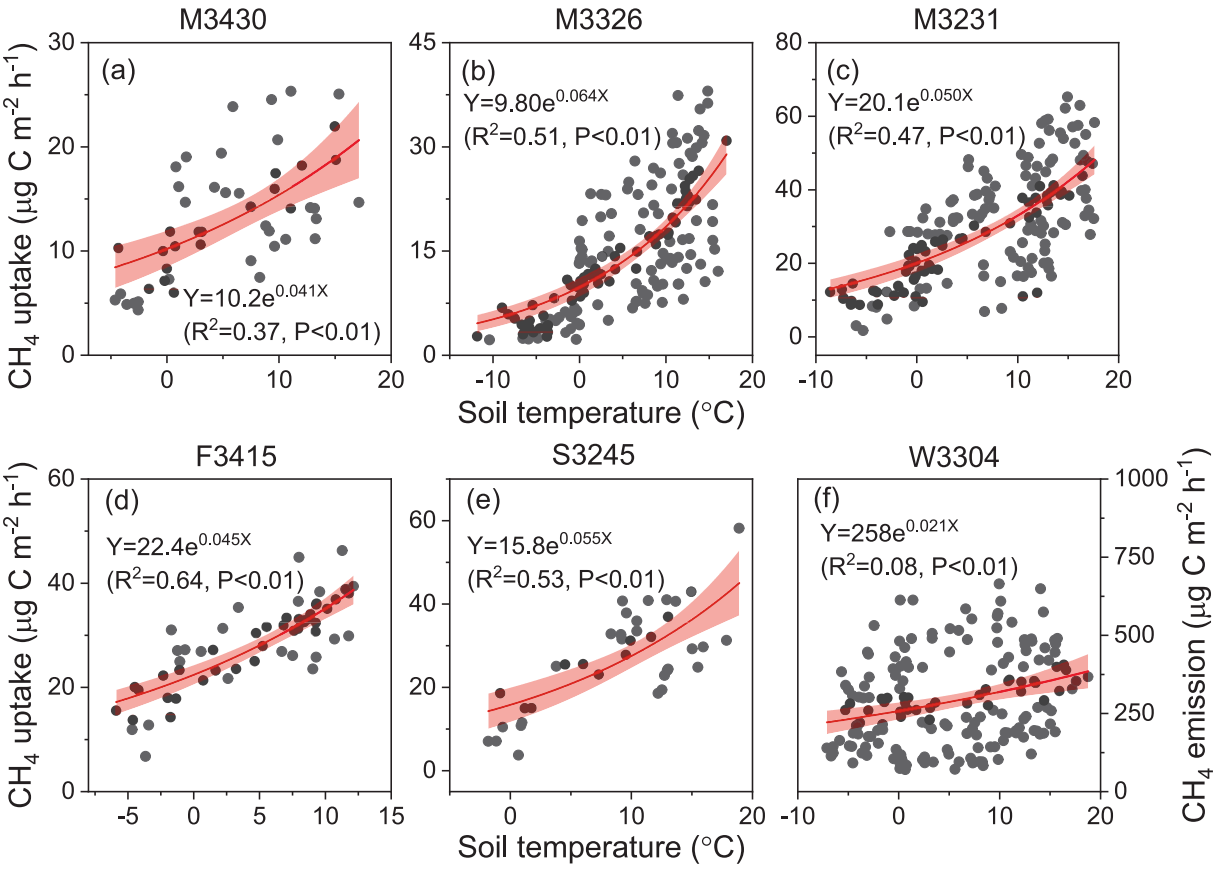

Fig. 3. Relationships between (a-e) methane (CH_4) uptake rates and soil temperature for alpine meadows at elevations of 3430 (M3430), 3326 (M3326) and 3231 m (M3231), forest at the elevation of 3415 m (F3415) and steppe at the elevation of 3245 m (S3245), respectively, and (f) CH_4 emissions and soil temperature for alpine wetland at the elevation of 3304 m (W3304). Shaded areas represent 95 % confidence bands.

18 to 45 % (Fig. S2).

3.3. Landscape patterns of annual CH_4 fluxes

Annual CH_4 uptake rates for all alpine upland sites ranged from 1.12 to 2.49 kg C ha^{-1} yr^{-1}, consisting of 0.71–1.59 kg C ha^{-1} and 0.41–0.94 kg C ha^{-1} for the growing and non-growing seasons, respectively (Tables 1 and 2). Specifically, CH_4 uptake rates in the non-growing season accounted for 29–42 % of the annual budgets. Among the upland sites, alpine forest showed higher annual CH_4 uptake rates than the meadow sites at higher elevations (M3430 and M3326), but no significant differences when comparing with alpine steppe (S3245) or the meadow site at the lowest elevation (M3231). Across all the upland sites, multiple linear regression analysis showed that the combined effects of soil temperature and WFPS explained about 81 % of the variation in annual CH_4 uptake rates (Fig. 7). However, soil WFPS was the primary driver of the variation in annual CH_4 uptake, and the significant relationship between them fits a quadratic regression. When the forest sites were excluded and only alpine grassland sites (M3430, M3326, S3245 and M3231) were considered, annual CH_4 uptake rates decreased significantly with increasing elevation (Fig. 7). For all the grassland sites, we also found a significant negative relationship between annual CH_4 uptake rates and soil N availability (here the relative proportion of NO_3^- in the total inorganic N pool was used as an indicator of soil N availability, as described by Davidson and Verchot, 2000).

Annual CH_4 emissions at alpine wetland sites varied from 17.2 to 34.3 kg C ha^{-1} yr^{-1}, of which approximately 38–46 % occurred during the non-growing season (Tables 1 and 2). Among the three microtopographies (W3304-H, W3304-T and W3304-W), there was no significant difference in either seasonal or annual CH_4 emissions. Across all alpine wetland sites and study years, the annual CH_4 emissions were positively correlated with WFPS (Fig. 8). Although the correlation with soil temperature alone was not statistically significant, adding this factor to the WFPS model significantly improved the estimation accuracy, explaining 95 % of the variation in annual CH_4 emissions. We also found a significant positive relationship between annual CH_4 emissions and soil inorganic N ($NH_4^+ + NO_3^-$) content.

Over the two-year measurements, annual CH_4 fluxes showed interannual variations for alpine ecosystems. That is, annual CH_4 emissions at the W3304 sites during the normal rainfall year (2013–2014) were almost twice as high as emissions during the drier year of 2014–2015 (Table 1). In contrast, annual CH_4 uptake rates at sites M3326 and M3231 were relatively higher in 2014–2015 compared with 2013–2014. Across all alpine upland and wetland sites within the landscape, the spatial pattern of annual CH_4 fluxes was mainly regulated by the variations in soil WFPS and inorganic N (NH_4^+ and NO_3^-) concentrations as well as their combined effects with soil temperature (Fig. 9). Moreover, model selection analysis based on Akaike weights emphasized the significance of soil inorganic N and WFPS in explaining the spatial variations of annual CH_4 fluxes from alpine upland and wetland ecosystems (Fig. S3). Taking into account the areal extent of the different alpine ecosystems, the landscape-scale CH_4 balance was a net sink of 0.72 kg C ha^{-1} yr^{-1} on average (Table 3).

4. Discussion

4.1. Temporal variations and driving forces of alpine ecosystem CH_4 fluxes

Our observations over a period of 2-years show that all alpine upland

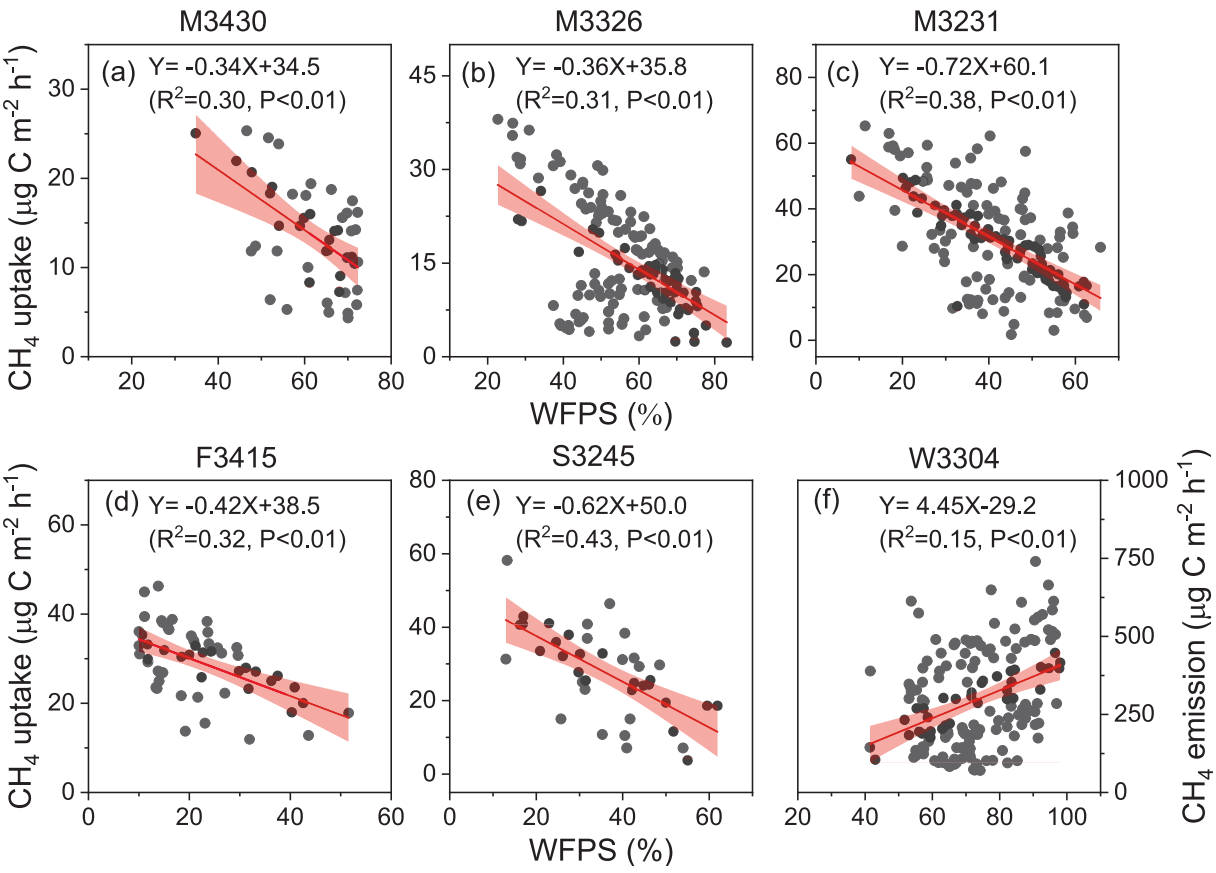

Fig. 4. Relationships between (a-e) methane (CH_4) uptake rates and soil water-filled pore space (WFPS) for alpine meadows at elevations of 3430 (M3430), 3326 (M3326) and 3231 m (M3231), forest at the elevation of 3415 m (F3415) and steppe at the elevation of 3245 m (S3245), respectively, and (f) CH_4 emissions and soil WFPS for alpine wetland at the elevation of 3304 m (W3304). Shaded areas represent 95 % confidence bands.

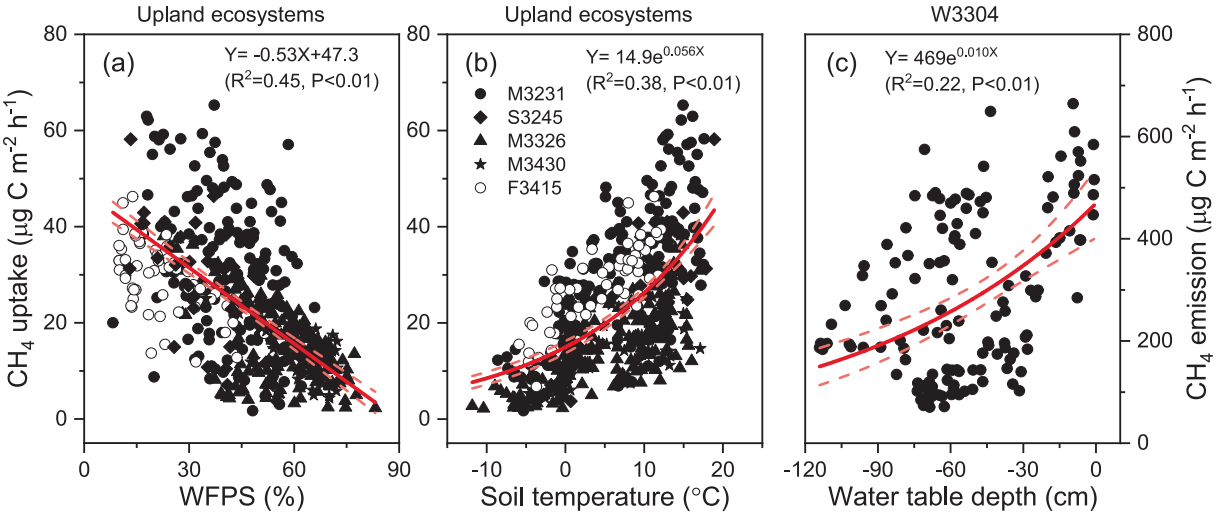

Fig. 5. Relationships between (a-b) methane (CH_4) uptake rates and water-filled pore space (WFPS) and soil temperature across all the upland ecosystems (including alpine meadows at elevations of 3430 (M3430), 3326 (M3326) and 3231 m (M3231), forest at the elevation of 3415 m (F3415) and steppe at the elevation of 3245 m (S3245)) and (c) CH_4 emissions and water table depth for alpine wetland at the elevation of 3304 m (W3304). Dashed lines represent 95 % confidence bands.

sites (M3430, F3415, M3326, S3245 and M3231) were characterized by a consistent net sink of CH_4 with different uptake rates, whereas alpine wetlands at the altitude of 3304 m (W3304) acted as net CH_4 emission sources (Figs. 1 and 2). Interestingly, CH_4 fluxes showed a similar seasonality in all alpine ecosystems studied, regardless of their CH_4 sink or source function. That is, high CH_4 uptake rates or emissions usually occurred during the growing season with relatively higher temperatures. Rates of both soil CH_4 uptake and emission have been reported to increase with increasing soil temperature in laboratory incubations (e.g., Bowden et al., 1998; Wu et al., 2010) and in field studies spanning grasslands (e.g., Mosier et al., 1996; Chen et al., 2011; Fu et al., 2018), forests (e.g., Steinkamp et al., 2001; Ishizuka et al., 2009; Ueyama et al.,

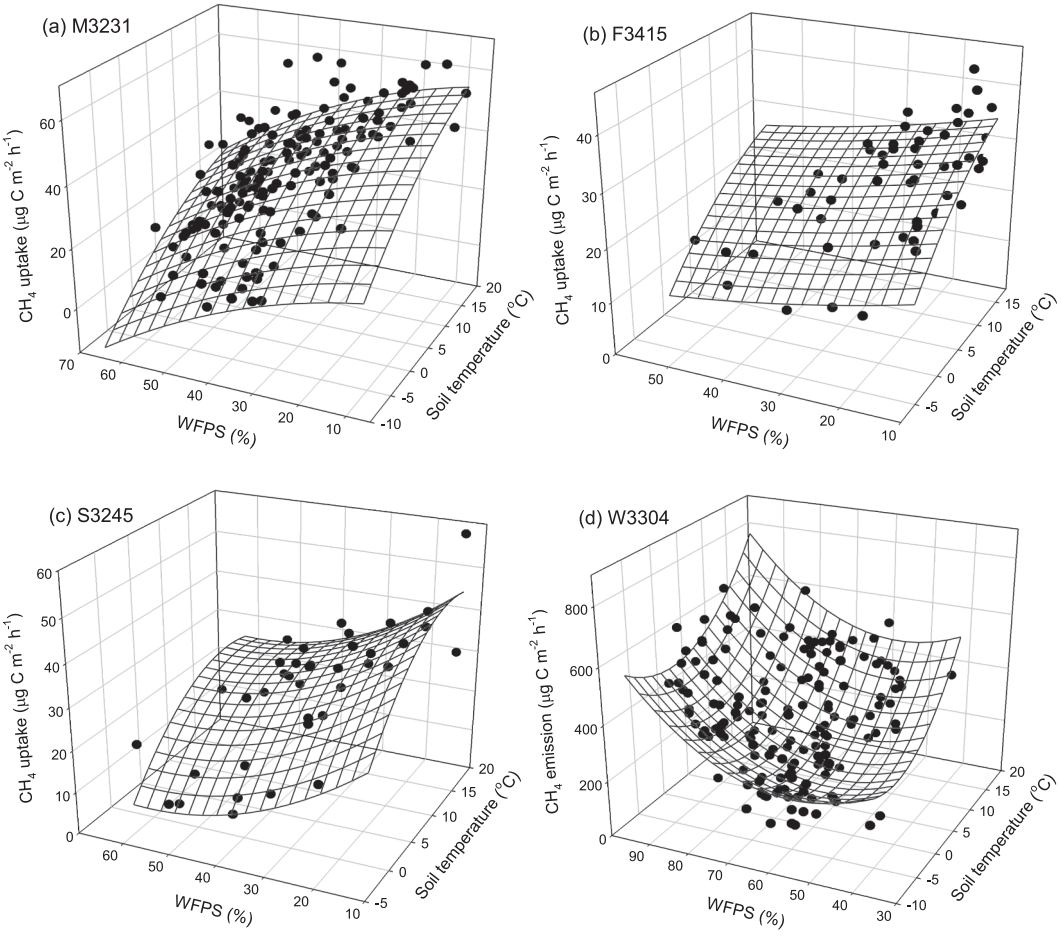

Fig. 6. Relationships between (a-c) methane (CH_4) uptake rates and the combined effect of soil temperature and water-filled pore space (WFPS) for alpine meadow at the elevation of 3231 m (M3231), forest at the elevation of 3415 m (F3430) and steppe at the elevation of 3245 m (S3245), respectively, and (d) CH_4 emissions and the combined effect of soil temperature and WFPS for alpine wetland at the elevation of 3304 m (W3304). The mesh plots are the result of multiple regression analysis in terms of the equations presented in Table S3.

2015) and wetlands (e.g., Song et al., 2015; Helbig et al., 2017). Similar to these previous studies, we observed that soil temperature was a significant predictor of CH_4 fluxes at both alpine upland and wetland sites, where the relationship was positive (Figs. 3 and 5). The change in soil temperature may have influenced not only CH_4 consumption by promoting methanotroph activities at the upland sites but also CH_4 production by stimulating microbial methanogenesis at the alpine wetland sites, and the associated CH_4 transport between soils and the atmosphere (Hosono and Nouchi, 1997; Song et al., 2015; Kaiser et al., 2018). The study also showed the temperature sensitivity of net CH_4 uptake or emission for the alpine ecosystems, with the Q_{10} values ranging from 1.23 to 1.90 (Table S2). These Q_{10} values are similar to those reported for other alpine ecosystems on the Tibetan Plateau (Q_{10}: 1.1–1.8, Guo et al., 2015; Fu et al., 2018), and fall within the range reported for temperate semiarid grasslands (Q_{10}: 1.4–2.1, Chen et al., 2011; Rong et al., 2015). Nevertheless, our Q_{10} values for CH_4 emissions from alpine wetlands were relatively lower than those for alpine uplands (mean: 1.23 vs. 1.75), suggesting a lower sensitivity of CH_4 fluxes from alpine wetlands to climate warming. This may be related to the high-water content, especially during the monsoon summer at alpine wetland sites. Soils with higher water content do have a high thermal buffering capacity, so that the temperature changes are rather small, and the consequent effects of temperature on microbial processes involved in CH_4 production. Although these alpine wetlands act as a buffer against increased temperatures, it is important to note that their feedback to ongoing climate change should not be ignored because their large soil organic C pool substantially affects the biogeochemical C cycle and associated CH_4 fluxes in high-altitude regions.

In addition to soil temperature, WFPS strongly influences on soil gas diffusion and microbial populations that drive the CH_4 dynamics (Potter et al., 1996; Smith et al., 2003; Koyama et al., 2024). Furthermore, the differential response of methanotrophs and methanogens to soil hydrology both between and within individual ecosystems can lead to differences in the correlation between CH_4 fluxes and soil WFPS (Luo et al., 2013; Kaiser et al., 2018). This finding is confirmed by the significant negative correlation between CH_4 uptake rates and WFPS in alpine uplands, and the positive regulation of CH_4 emissions by WFPS in alpine wetlands (Fig. 4). The CH_4 emissions from alpine wetlands were also positively correlated with WTD, which is consistent with many previous studies (Olefeldt et al., 2013; Turetsky et al., 2014; Song et al., 2015). The opposite response of CH_4 fluxes to soil moisture status between alpine upland and wetland sites was likely because higher WFPS could suppress gas diffusion and increase anaerobic soil volume, which would suppress methanotrophy and stimulate methanogenesis, thus, reducing CH_4 oxidation and promoting CH_4 production (Wei et al., 2015; Yu et al., 2019; Koyama et al., 2024). On the other hand, our study suggested that the temporal variations of CH_4 fluxes in all alpine ecosystems could be explained by the combined effects of soil temperature and WFPS, which is beyond the effects of soil temperature or WFPS alone (Fig. 6). The parameters given by our fits can provide insights for the improvement of mechanistic (process-based) or empirical (data-driven) models to fully account for the dynamics of terrestrial CH_4

Table 2
Total cumulative methane (CH_4) uptake or emission (in kg C ha^{-1}) across the growing season and non-growing season as well as the non-growing season contribution to annual budgets for different ecosystem sites along the elevation gradient in a Tibetan alpine landscape over the period 2013–2015.

Year	Ecosystem type	Growing season	Non-growing season (NGS)	NGS contribution to annual budget
Upland sites				
2013–2014	M3430	0.71 ± 0.04c	0.41 ± 0.04b	37 %
	M3326	1.00 ± 0.04b	0.42 ± 0.01b	29 %
	M3231	1.47 ± 0.04 a	0.86 ± 0.05 a	37 %
2014–2015	F3415	1.31 ± 0.11 ab	0.94 ± 0.04 a	42 %
	M3326	1.08 ± 0.02b	0.54 ± 0.04b	33 %
	S3245	1.53 ± 0.06 a	0.67 ± 0.07b	30 %
	M3231	1.59 ± 0.03 a	0.91 ± 0.02 a	36 %
Wetland sites				
2013–2014	W3304-H	18.6 ± 6.2 a	11.3 ± 3.5 a	38 %
	W3304-T	19.6 ± 6.2 a	14.1 ± 3.6 a	42 %
	W3304-W	20.6 ± 8.8 a	13.7 ± 4.1 a	40 %
	Area-weighted	19.5 ± 6.4	13.5 ± 3.6	41 %
2014–2015	W3304-H	9.9 ± 3.8 a	7.4 ± 2.3 a	43 %
	W3304-T	9.5 ± 2.9 a	7.8 ± 2.6 a	45 %
	W3304-W	9.4 ± 4.9 a	8.1 ± 2.8 a	46 %
	Area-weighted	9.6 ± 3.2	7.7 ± 2.5	45 %

Values represent mean ± standard error (n = 4–6). ds, dry soil. Ecosystem types are coded as follows: M = alpine meadow; F = alpine forest; S = alpine steppe; W = alpine wetland; 6-digit numbers = elevation in m above sea level; micro-topographies of wetlands: −H = hummocks, −T = transition between micro-topographies, −W = hollow water holes. Area-weighted CH_4 emission was calculated in terms of the areal extent of 20 %, 71 % and 9 % for the W3304-H, W3304-T and W3304-W, respectively. Different letters within the same column indicate significant differences among the ecosystems in each year at the $P < 0.05$ level.

fluxes. Additionally, higher CH_4 fluxes during the growing season were likely related to the presence of vegetation and its driving mechanisms (Plain et al., 2019). For alpine upland sites, the vegetation growth may increase soil air permeability due to root penetration, which facilitates CH_4 uptake by enhancing the transport of CH_4 and O_2 into the soil and/or by promoting the growth of methanotrophic populations. In alpine wetlands, where CH_4 production prevails, the vegetation growth may instead enhance soil CH_4 emissions by increasing the availability of C substrates such as litters and root exudates. Overall, modeling soil CH_4 exchange in alpine ecosystems, particularly in the context of global climate change, requires consideration of the interactive effects of soil temperature and moisture content and vegetation's impact on CH_4 uptake rates or emissions.

4.2. *Landscape patterns and environmental controls of annual CH_4 fluxes*

For alpine uplands, annual CH_4 uptake was about 2.26 kg C ha^{-1} yr^{-1} for the forest site and varied from 1.12 to 2.49 kg C ha^{-1} yr^{-1} for grassland sites (Table 1). Our estimated annual CH_4 uptake was generally within the reported range for other alpine grasslands (1.3–4.2 kg C ha^{-1} yr^{-1}, He et al., 2014; Guo et al., 2015; Fu et al., 2018) and forests (2.1–5.2 kg C ha^{-1} yr^{-1}, Dong et al., 2003) in China. Based on field surveys and modeling studies, the average annual CH_4 uptake was estimated to be 0.82–3.34 and 0.75–3.59 kg C ha^{-1} yr^{-1} for global grasslands and forests, respectively (Curry, 2007; Dalal and Allen, 2008; Yu et al., 2017). For our alpine wetlands, annual CH_4 emissions were 17.2–34.3 kg C ha^{-1} yr^{-1}, which is at the lower end of the range (9.1–254 kg C ha^{-1} yr^{-1}) reported for other alpine wetlands in China (He et al., 2014; Song et al., 2015). Likewise, our annual CH_4 emission estimates were relatively lower than the mean value of 127 kg C ha^{-1} yr^{-1} for global wetlands (Dalal and Allen, 2008), or towards the lower end of the reported range for various wetlands of worldwide cold/cool biomes, such as temperate wetlands (2.1–394 kg C ha^{-1} yr^{-1}, Kang and Freeman, 2002; Song et al., 2009; Juszczak and Augustin, 2013; Olson et al., 2013; Hommeltenberg et al., 2014; Fortuniak et al., 2017), boreal wetlands (3.5–455 kg C ha^{-1} yr^{-1}, Whalen and Reeburgh, 1992; Rinne et al., 2007; Flessa et al., 2008; Nilsson et al., 2008; Leppälä et al., 2011; Li et al., 2016) and tundra wetlands (21.9–221 kg C ha^{-1} yr^{-1}, Wille et al., 2008; Jackowicz-Korczyński et al., 2010; Christiansen et al., 2012; Zona et al., 2016; Jammet et al., 2017). Given that the spatiotemporal heterogeneity of CH_4 fluxes was highly dependent on climate, soil properties, plant communities and site-specific management (e.g., West et al., 1999; Luo et al., 2013; Treat et al., 2018; D'Imperio et al., 2023), the reason for our low annual CH_4 emissions was likely related to the specific characteristics of Tibetan alpine wetlands. Specifically, more than 50 % of alpine wetlands on the Tibetan Plateau were seasonally inundated, mainly due to deliberate drainage for rangeland expansion over the past decades (Xiang et al., 2009; Zhang et al., 2019). As observed in our study, the drainage significantly lowered the wetland WTD, which likely altered the condition of the wetland from predominantly anaerobic to more aerobic, thereby reducing CH_4 emissions (Gan et al., 2024). These low CH_4 emissions were also consistent with observations from other drained wetlands in tropical, temperate or boreal zones, where much of the CH_4 produced deeper in the wetland soil was oxidized before reaching the soil surface (Couwenberg et al., 2010; Turetsky et al., 2014; Wilson et al., 2016; Kwon et al., 2017; Gan et al., 2024).

There is increasing evidence that the role of non-growing season CH_4 fluxes in the annual budget cannot be overlooked in cold climate regions (e.g., Mosier et al., 1996; Chen et al., 2011; Treat et al., 2018). However, studies on the important contributions of non-growing CH_4 fluxes are still limited in high-altitude regions such as the Tibetan Plateau, due to the harsh winter environment and technical limitations (Song et al., 2015; Fu et al., 2018; Peng et al., 2019). In this study, we show that the non-growing season CH_4 fluxes accounted for a significant proportion, ranging from 29 % to 46 % of the annual budgets in all alpine uplands and wetlands (Table 2). This suggests that even when the soil temperature dropped down to < 0 °C, the landscape elements on the Tibetan Plateau still persisted as an important and non-zero sink or source of atmospheric CH_4. Our results confirm and generalize previous findings (e.g., Sommerfeld et al., 1993; Butterbach-Bahl and Papen, 2002; Treat et al., 2018). As previous studies have suggested, a high fraction of non-growing season CH_4 fluxes is likely related to persistent biological production or consumption under winter snow cover, which acts as an insulator (Mast et al., 1998). Furthermore, warmer temperatures in deeper soil profiles may facilitate CH_4-related microbial processes, such as CH_4 oxidation in upland sites and CH_4 production in wetland sites, even when surface soils are colder or under unfavorable conditions during the winter time (Chen et al., 2011; Treat et al., 2018; Zhang et al., 2019). For regions with either continuous or discontinuous permafrost, the magnitude of non-growing CH_4 emissions was reported to be higher during the onset of freezing or during the spring freezing-thawing period (Mastepanov et al., 2008; Song et al., 2012). These high CH_4 emission pulses may result from the storage and subsequent release of previously produced CH_4 during the non-growing season, or from the interaction between soil temperature, vegetation and substrate availability, which can influence rates of CH_4 production and oxidation (Treat et al., 2018). Regarding our seasonally frozen sites, wetland CH_4 emissions did not demonstrate obvious pulses during freeze–thaw periods, accounting for only 12–16 % of total annual CH_4 emissions (Zhang et al., 2019). This may be related to the following: efficient vegetation-mediated CH_4

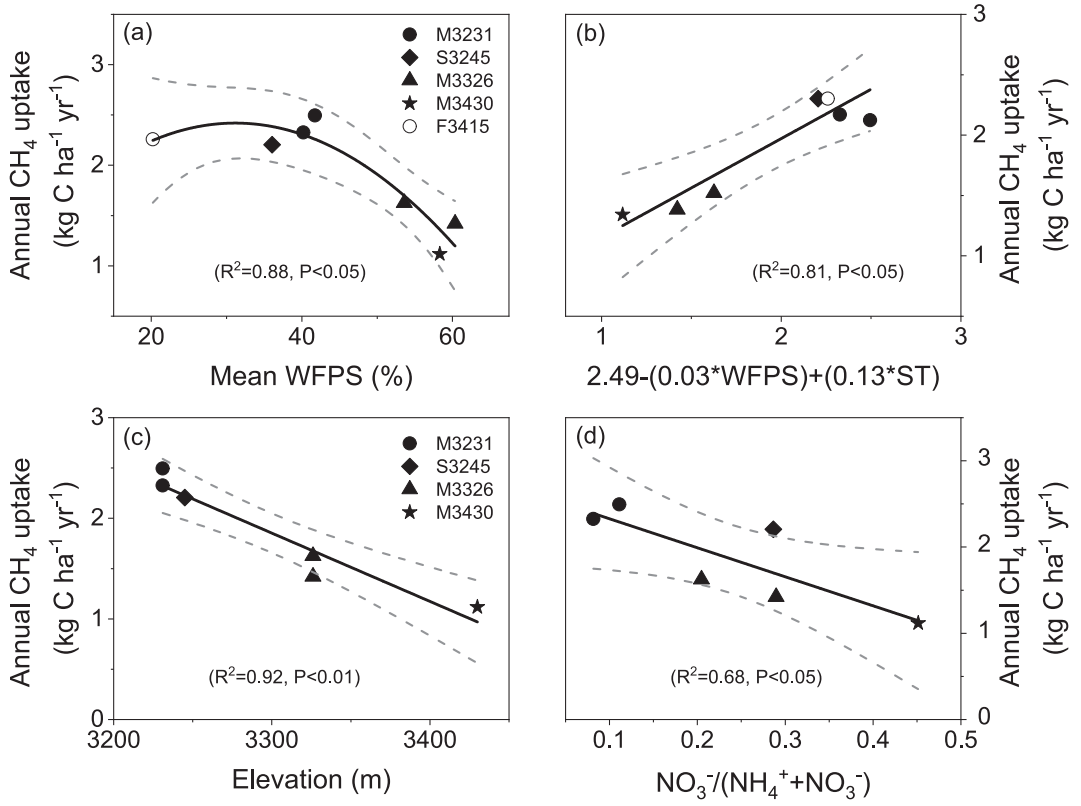

Fig. 7. Relationships between (a-b) annual methane (CH_4) uptake and mean soil water-filled pore space (WFPS) or the combined effect of WFPS (in %) and soil temperature (ST, in ℃) across all the alpine upland ecosystems (including alpine meadows at elevations of 3430 (M3430), 3326 (M3326) and 3231 m (M3231), forest at the elevation of 3415 m (F3415) and steppe at the elevation of 3245 m (S3245)), and (c-d) annual CH_4 uptake against the elevation gradient or the ratio of nitrate (NO_3^-) to soil inorganic N pool ($NH_4^+ + NO_3^-$) across all the alpine grasslands (i.e., M3430, M3326, S3245 and M3231). Dashed lines represent 95 % confidence bands.

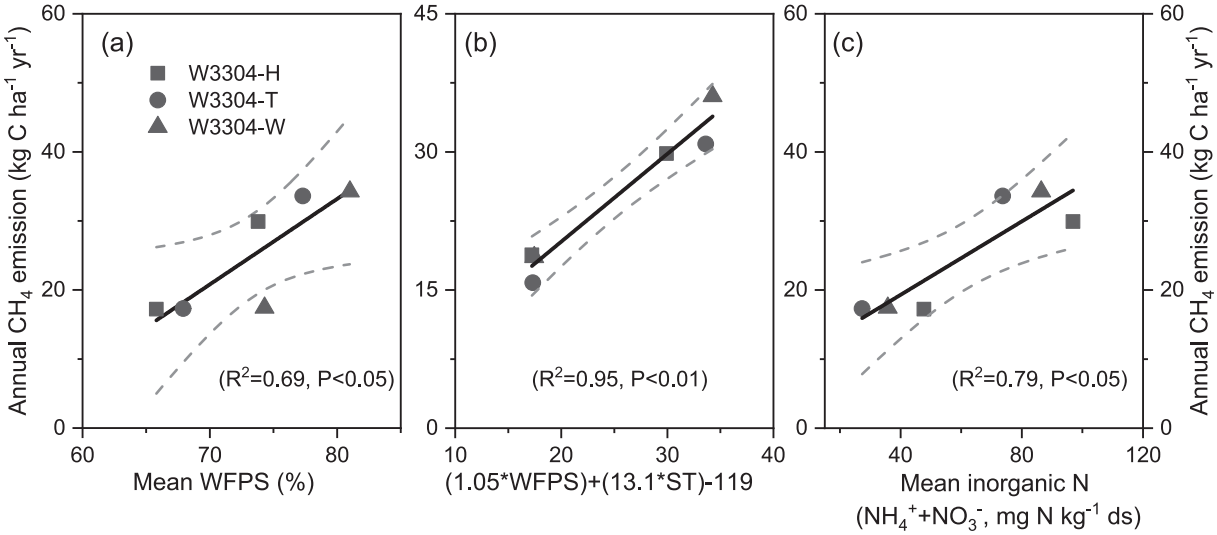

Fig. 8. Relationships between (a-c) annual methane (CH_4) emissions and mean water-filled pore space (WFPS), the combined effect of WFPS (in %) and soil temperature (ST, in ℃) or mean inorganic N pool ($NH_4^+ + NO_3^-$) across all the micro-topographies (i.e., −H = hummocks, −T = transition between micro-topographies, −W = hollow water holes) of alpine wetlands at the elevation of 3304 m (W3304). Dashed lines represent 95 % confidence bands.

emissions which reduce the role of storage within the subsurface; weak thaw-initiated microbial CH_4 production; and the absence of a permafrost bottom (Mastepanov et al., 2008; Song et al., 2012; Song et al., 2015; Zhang et al., 2019). However, given that non-growth season processes are critical for accurate estimation of annual CH_4 fluxes from high-elevation ecosystems, it is imperative for future research to conduct year-round measurements, especially with high temporal and spatial coverage.

Another important finding of this study is that we evaluated the spatial patterns of annual CH_4 fluxes across the Tibetan alpine landscape. Although it has long been known that soil temperature, moisture, and C and N availability affect CH_4 fluxes across heterogeneous landscapes (e.g., West et al., 1999; Olefeldt et al., 2013; Kaiser et al., 2018; Yu et al., 2019), our results corroborated that these variables were the

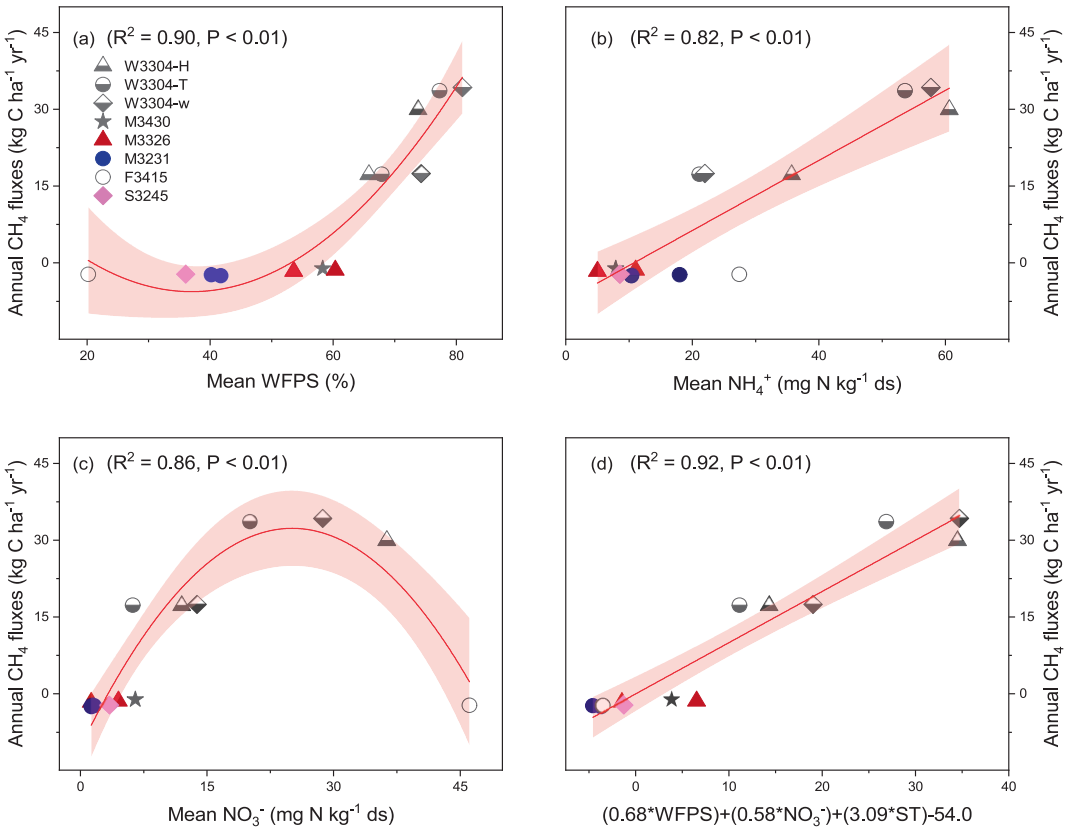

Fig. 9. Relationships between (a-d) annual methane (CH_4) fluxes and mean water-filled pore space (WFPS), soil ammonium (NH_4^+) and nitrate (NO_3^-) concentrations and the combined effect of WFPS (in %), NO_3^- (in mg N kg^{-1} ds) and soil temperature (ST, in °C) across all different ecosystems along the elevation gradient within the Tibetan alpine landscape. Ecosystem types are coded as follows: M = alpine meadow; F = alpine forest; S = alpine steppe; W = alpine wetland; 6-digit numbers = elevation in m above sea level; micro-topographies of wetlands: −H = hummocks, −T = transition between micro-topographies, −W = hollow water holes. Shaded areas represent 95 % confidence bands.

main controls of annual CH_4 fluxes among different landscape elements on the Tibetan Plateau. Based on single-factor correlation analysis, our empirical model shows that WFPS was the most dominant factor controlling CH_4 uptake in alpine uplands, whereas inorganic N (NH_4^+ + NO_3^-) content was the dominant factor controlling CH_4 emissions in alpine wetlands (Figs. 7a and 8c). Nevertheless, our analysis stresses WFPS as the primary control of annual CH_4 fluxes in all alpine ecosystems. Soil temperature did not show a significant relationship with annual CH_4 uptake or emissions, but instead resulted in a positive control of CH_4 fluxes when interacting with WFPS and soil inorganic N. As mentioned above, that higher WFPS corresponded to less CH_4 uptake and more CH_4 emissions was often associated with its influence on microbial activity and soil diffusivity (e.g., Smith et al., 2003; Yu et al., 2019; Koyama et al., 2024). The significant influence of WFPS on CH_4 oxidation or CH_4 production was also reflected in the interannual CH_4 flux patterns, as observed at sites M3326, M3231 and W3304. The inclusion of soil temperature in the WFPS model may be due to the influence of soil hydrology on soil temperature by controlling thermal conductivity. However, it is challenging to elucidate the possible mechanisms behind the correlation between soil inorganic N and CH_4 fluxes because high N availability does not always reduce CH_4 uptake and promote CH_4 emission through direct competitive inhibition of CH_4 oxidation or by a stimulation of methanogenesis (Aronson and Helliker, 2010; Hofmann et al., 2016; Koyama et al., 2024). As expected, many studies have reported mixed results, including positive, negative and no significant correlations between CH_4 fluxes and soil inorganic N (NH_4^+, NO_3^- or NH_4^+ + NO_3^-) content in forests, grasslands and peatlands (Cen et al., 2024; Goldman et al., 1995; Reay et al., 2001; Tate et al., 2007; Zhao and Zhuang, 2024). Additionally, soil organic matter is an important factor in regulating ecosystem CH_4 fluxes because it can provide C substrates to methanogens and methanotrophs and enhance their activities by stimulating growth (Yu et al., 2017; Lee et al., 2023). Although our model selection analysis based on Akaike weights did not demonstrate the significance of soil organic C on spatial variations of annual CH_4 fluxes across alpine upland and wetland ecosystems, analyzing the composition of soil organic C (e.g., particulate and mineral-associated organic C) and microbial activity and community composition may help explain variations in ecosystem CH_4 fluxes (Lee et al., 2023; Han et al., 2024). Further exploration of this topic is required in future studies.

4.3. *Net CH_4 budget of a Tibetan alpine landscape*

For the studied Tibetan alpine landscape, its area was dominated by large proportions of alpine uplands including alpine meadow, steppe and forest, while 4.6 % of the total area was characterized by alpine wetlands. As suggested by several studies (e.g., D'Imperio et al., 2017; Bernhardt et al., 2017; Kaiser et al., 2018), it is critically important to perform the landscape-scale analysis to determine the relative impact of site-scale measurements on the net landscape balance. Based on the cumulative CH_4 fluxes and areal contributions of different landscape elements, we estimated the landscape-scale net annual CH_4 budget (Table 3). Despite the relatively small area of alpine wetlands, their CH_4 emissions could negate up to 62 % of the upland CH_4 uptake. On average, the landscape-scale CH_4 budget was a net CH_4 sink with a magnitude of 0.72 ± 0.43 kg C ha^{-1} yr^{-1}. On the other hand, both alpine uplands and wetlands within this Tibetan landscape were reported to be net sources of N_2O (ranging from 0.05-1.06 kg N ha^{-1} yr^{-1}, Yao et al.,

Table 3
Estimated the landscape-scale (area-weighted) annual methane (CH_4) and nitrous oxide (N_2O) fluxes and the related total CH_4 and non-CO_2 greenhouse gas (GHG) budgets across the total Tibetan alpine landscape area (including all meadow, steppe, forest and wetland areas on the Tibetan Plateau).

Ecosystem type	Area (ha)	Percent (%)	Mean annual CH_4 fluxes (kg C ha^{-1} yr^{-1})	Mean annual N_2O emissions (kg N ha^{-1} yr^{-1})
M3430	29	15.3	−1.12 ± 0.08	0.05 ± 0.01
F3415	44	23.1	−2.26 ± 0.11	0.77 ± 0.22
M3326	38	20.1	−1.52 ± 0.05	0.15 ± 0.04
W3304	9	4.6	25.1 ± 7.8	1.06 ± 0.63
S3245	14	7.1	−2.21 ± 0.11	0.19 ± 0.03
M3231	56	29.8	−2.41 ± 0.07	0.17 ± 0.02
Landscape-scale (Area-weighted) [a]	189	100	−0.72 ± 0.43	0.33 ± 0.10
Total alpine landscape area across the Tibetan Plateau [b]	1590.33 × 10^3 km^2			
Total CH_4 flux across the total Tibetan alpine landscape area	−0.15 ± 0.07 Tg CH_4 yr^{-1}			
Non-CO_2 GHG (CH_4 + N_2O) flux across the total Tibetan alpine landscape area	18.2 ± 4.1 Tg CO_2-eq yr^{-1}			

Values represent mean ± standard error (n = 4–6). Ecosystem types are coded as follows: M = alpine meadow; F = alpine forest; S = alpine steppe; W = alpine wetland; 6-digit numbers = elevation in m above sea level. Negative and positive values represent soil fuction as sinks and sources for atmospheric CH_4, respectively. [a] Landscape-scale (area-weighted) annual CH_4 and N_2O flux is estimated by the areal extent of individual land use/cover types within the Tibetan alpine landscape, here the data for annual N_2O emissions from different alpine ecosystems were adopted from our published work (Yao et al., 2022). [b] Total Tibetan alpine landscape area is estimated by the sum of all meadow, steppe, forest and wetland areas on the Tibetan Plateau (Chen et al., 2022).

2022), resulting in a landscape-scale net annual N_2O budget of 0.33 ± 0.10 kg N ha^{-1} yr^{-1} (Table 3). By aggregating CH_4 uptake and N_2O emission through their global warming potential indices of 27 (for CH_4) and 273 (for N_2O) on the centennial scale (IPCC, 2021), the net landscape-scale non-CO_2 GHG flux was calculated to be 115 ± 26 kg CO_2-eq ha^{-1} yr^{-1}. This suggests that annual N_2O emissions outweigh the climate benefits of the net landscape-scale CH_4 sink.

The landscape-scale assessment conducted in this study is relevant to the Tibetan Plateau as a whole, where the topography and landscape elements are the similar to those of our studied alpine landscape (Chen et al., 2022). Accordingly, we further conducted total CH_4 and non-CO_2 GHG budgets for the entire Tibetan Plateau by multiplying the total area of the Tibetan alpine landscape (including all meadow, steppe, forest and wetland areas). Our preliminary estimate indicates that alpine terrestrial ecosystems across the Tibetan Plateau are a weak CH_4 sink (with 0.15 ± 0.07 Tg CH_4 yr^{-1}) but a net source of non-CO_2 GHG (CH_4 + N_2O) emission (with 18.2 ± 4.1 Tg CO_2-eq yr^{-1}) (Table 3). This is in good agreement with the estimation by Chen et al. (2024) for the net CH_4 budget of all alpine terrestrial ecosystems in the same region (net CH_4 sink of 0.20 Tg CH_4 yr^{-1}, 95 % confidence interval: 0.01–0.34 Tg CH_4 yr^{-1}). Nevertheless, we readily acknowledge that our upscaling estimate may have been constrained by the dataset structure of the observations, resulting in some uncertainties and limitations. If we are to further improve its representativeness, more field measurements spanning better temporal distributions and covering various landscape scales are needed to be done in the future. Given that alpine uplands and wetlands on the Tibetan Plateau are extremely vulnerable and sensitive to climate change (Liu et al., 2018), the future warmer and wetter climate in this region (Wang et al., 2023) may alter the net CH_4 sink. For instance, warming-induced permafrost thawing as well as increased precipitation on the Tibetan Plateau may subject alpine terrestrial ecosystems to more anaerobic conditions, and thereby triggering substantial CH_4 release to the atmosphere (Chen et al., 2024), indicating the vulnerability of alpine landscape CH_4 balances from a net CH_4 sink to become a net CH_4 source under future climate change. Such feedbacks from the Tibetan alpine landscapes and other similar high-altitude ecosystems will pose a challenge to the Paris Agreement, which requires large efforts to reduce soil CH_4 emissions for achieving its goals.

5. Conclusions

This study provides insights into the spatial and temporal patterns of CH_4 fluxes from major landscape elements on the Tibetan Plateau: alpine meadow, steppe, forest and wetland. Our results show that the seasonal variations of CH_4 fluxes at individual alpine upland and wetland sites are highly dependent on the interactions between soil temperature and soil water content. Despite the harsh winter environment, which is often assumed to suppress microbial activities and associated CH_4 fluxes, our study highlights the significance of non-growing season CH_4 fluxes for accurate estimation of annual CH_4 budgets in high-altitude ecosystems. Moreover, our results suggest that soil hydrological status (or the combined effect of soil moisture and temperature) and soil inorganic N content are the main factors regulating the landscape patterns of annual CH_4 fluxes in all alpine uplands and wetlands. Based on annual CH_4 fluxes and the areal contribution of landscape elements, we show that although CH_4 emissions from alpine wetlands can contribute disproportionally to annual CH_4 balances, their much smaller area relative to the alpine uplands made the studied landscape remain a net sink of atmospheric CH_4. However, with the projected warmer and wetter climate in the future, the amount of CH_4 emissions from alpine terrestrial ecosystems may increase, and potentially turn these Tibetan Plateau landscapes to net sources of atmospheric CH_4.

CRediT authorship contribution statement

Zhisheng Yao: Writing – review & editing, Writing – original draft, Project administration, Investigation, Data curation, Conceptualization. **Rui Wang:** Methodology, Investigation, Data curation. **Han Zhang:** Methodology, Investigation, Data curation. **Lei Ma:** Investigation, Formal analysis, Data curation. **Xunhua Zheng:** Writing – review & editing, Project administration, Funding acquisition, Conceptualization. **Kai Wang:** Methodology, Investigation. **Wei Zhang:** Investigation, Data curation. **Yong Li:** Writing – review & editing, Resources, Project administration. **Bo Zhu:** Writing – review & editing, Resources. **Klaus Butterbach-Bahl:** Writing – review & editing, Resources, Project administration, Conceptualization.

Declaration of competing interest

The authors declare that they have no known competing financial interests or personal relationships that could have appeared to influence the work reported in this paper.

Acknowledgements

This work was supported by the National Natural Science Foundation of China (41977282, 42177217 and 42161144002,) and the National Key Research and Development Program of China (2012CB417100). We are also thankful for Yanqiang Wang, Xiaolong Wang, Shenghui Han and Lei Li for their investigation and sampling in the field and laboratory.

Appendix A. Supplementary data

Supplementary data to this article can be found online at https://doi.org/10.1016/j.geoderma.2025.117523.

Data availability

Data will be made available on request.

References

Anderson, T., Groffman, P., Walter, M., 2015. Using a soil topographic index to distribute denitrification fluxes across a northeastern headwater catchment. J. Hydrol. 522, 123–134.

Aronson, E., Helliker, B., 2010. Methane flux in non-wetland soils in response to nitrogen addition: a meta-analysis. Ecology 91, 3242–3251.

Bernhardt, E., Blaszczak, J., Ficken, C., Fork, M., Kaiser, K., Seybold, E., 2017. Control Points in Ecosystems: moving beyond the Hot Spot Hot Moment Concept. Ecosystems 20, 665–682.

Bowden, R., Newkirk, K., Rullo, G., 1998. Carbon dioxide and methane fluxes by a forest soil under laboratory-controlled moisture and temperture conditions. Soil Biol. Biochem. 30, 1591–1597.

Bridgham, S., Cadillo-Quiroz, H., Keller, J., Zhuang, Q., 2013. Methane emissions from wetlands: Biogeochemical, microbial, and modeling perspective from local to global scales. Glob. Chang. Biol. 19, 1325–1346.

Butterbach-Bahl, K., Papen, H., 2002. Four years continuous record of CH4-exchange between the atmosphere and untreated and limed soil of a N-saturated spruce and beech forest ecosystem in Germany. Plant and Soil 240, 77–90.

Cen, X., He, N., Li, M., Xu, L., Yu, X., Cai, W., Li, X., Butterbach-Bahl, K., 2024. Suppression of nitrogen deposition on global forest soil CH4 uptake depends on nitrogen status. Global Biogeochem. Cycles 38, e2024GB008098.

Chen, H., Ju, P., Zhu, Q., Xu, X., Wu, N., Gao, Y., Feng, X., Tian, J., Niu, S., Zhang, Y., Peng, C., Wang, Y., 2022. Carbon and nitrogen cycling on the Qinghai-Tibetan Plateau. Nat. Rev. Earth Environ. 3, 701–716.

Chen, H., Yao, S., Wu, N., Wang, Y., Luo, P., Tian, J., Gao, Y., Sun, G., 2008. Determinants influencing seasonal variations of methane emissions from alpine wetlands in Zoige Plateau and their implications. J. Geophys. Res. Atmos. 113, D12303.

Chen, L., Yang, G., Bai, Y., Chang, J., Qin, S., Liu, F., He, M., Song, Y., Zhang, F., Peñuelas, J., Zhu, B., Zhou, G., Yang, Y., 2024. Permafrost carbon cycle and its dynamics on the Tibetan Plateau. Sci. China Life Sci. 67, 1833–1848.

Chen, W., Wolf, B., Zheng, X., Yao, Z., Butterbach-Bahl, K., Brüggemann, N., Liu, C., Han, S., Han, X., 2011. Annual methane uptake by temperate semiarid steppes as regulated by stocking rates, aboveground plant biomass and topsoil air permeability. Glob. Chang. Biol. 17, 2803–2816.

Christiansen, J.R., Gundersen, P., Vesterdal, L., 2012. Nitrous oxide and methane exchange in two small temperate forest catchments—effects of hydrological gradients and implications for global warming potentials of forest soils. Biogeochemistry 107, 437–454.

Conrad, R., 1996. Soil microorganisms as controllers of atmospheric trace gases (H2, CO, CH4, OCS, N2O, and NO). Microbiol. Rev. 60, 609–640.

Couwenberg, J., Dommain, R., Joosten, H., 2010. Greenhouse gas fluxes from tropical peatlands in south–east Asia. Glob. Chang. Biol. 16, 1715–1732.

Creed, I., Trick, C., Band, L., Morrison, I., 2002. Characterizing the spatial pattern of soil carbon and nitrogen pools in the Turkey Lakes Watershed: a comparison of regression techniques. Water Air Soil Pollut. 2, 81–102.

Curry, C.L., 2007. Modeling the soil consumption of atmospheric methane at the global scale. Global Biogeochem. Cycles 21, GB4012.

D'Imperio, L., Li, B., Tiedje, J., Oh, Y., Christiansen, J., Kepfer-Rojas, S., Westergaard-Nielsen, A., Brandt, K., Holm, P., Wang, P., Ambus, P., Elberling, B., 2023. Spatial controls of methane uptake in upland soils across climatic and geological regions in Greenland. Commun. Earth Environ. 4, 461.

D'Imperio, L., Nielsen, C., Westergaard-Nielsen, A., Michelsen, A., Elberling, B., 2017. Methane oxidation in contrasting soil types: responses to experimental warming with implication for landscape-integrated CH4 budget. Glob. Chang. Biol. 23, 966–976.

Dalal, R.C., Allen, D.E., 2008. Greenhouse gas fluxes from natural ecosystems. Aust. J. Bot. 56, 369–407.

Davidson, E.A., Verchot, L.V., 2000. Testing the Hole-in-the-Pipe model of nitric and nitrous oxide emissions from soils using the TRAGENT Database. Global Biogeochem. Cycles 14, 1035–1043.

Dong, Y., Qi, Y., Lou, J., Liang, T., Luo, K., Zhang, S., 2003. Experimental study on N2O and CH4 fluxes from the dark coniferous forest zone soil of the Gongga Mountain, China. Sci. China (series d) 46, 285–295.

Duncan, J., Groffman, P., Band, L., 2013. Towards closing the watershed nitrogen budget: Spatial and temporal scaling of denitrification. J. Geophys. Res. Biogeo. 118, 1105–1119.

Feng, Z., Xu, Y., Kobayashi, K., Dai, L., Zhang, T., Agathokleous, E., Calatayud, V., Paoletti, E., Mukherjee, A., Agrawal, M., Park, R., Oak, Y., Yue, X., 2022. Ozone pollution threatens the production of major staple crops in East Asia. Nat. Food 3, 47–56.

Flessa, H., Rodionov, A., Guggenberger, G., Fuchs, H., Magdon, P., Shibistova, O., Zrazhevskaya, G., Mikheyeva, N., Kasansky, O., Blodau, C., 2008. Landscape controls of CH4 fluxes in a catchment of the forest tundra ecotone in northern Siberia. Glob. Chang. Biol. 14, 1–17.

Fortuniak, K., Pawlak, W., Bednorz, L., Grygoruk, M., Siedlecki, M., Zieliński, M., 2017. Methane and carbon dioxide fluxes of a temperate mire in Central Europe. Agric. For. Meteorol. 232, 306–318.

Fu, B., Li, J., Jiang, Y., Chen, Z., Li, B., 2024. Clean air policy makes methane harder to control due to longer lifetime. One Earth 7, 1266–1274.

Fu, Y., Liu, C., Lin, F., Hua, X., Zheng, X., Zhang, W., Cao, G., 2018. Quantification of year–round methane and nitrous oxide fluxes in a typical alpine shrub meadow on the Qinghai–Tibetan Plateau. Agric. Ecosyst. Environ. 255, 27–36.

Gan, D., Zhang, Z., Li, H., Yu, D., Li, Z., Long, R., Niu, S., Zuo, H., Meng, X., Wang, J., Ma, L., 2024. Ditch emissions partially offset global reductions in methane emissions from peatland drainage. Commun. Earth Environ. 5, 640.

Gauthier, M., Bradley, R., Šimek, M., 2015. More evidence that anaerobic oxidation of methane is prevalent in soils: is it time to upgrade our biogeochemical models? Soil Biol. Biochem. 80, 167–174.

Goldman, M., Groffman, P., Pouyat, R., McDonnell, M., Pickett, S., 1995. CH4 uptake and N availability in forest soils along an urban to rural gradient. Soil Biol. Biochem. 27, 281–286.

Guo, X., Du, Y., Han, D., Xu, X., Zhang, F., Lin, L., Li, Y., Liu, S., Ouyang, J., Cao, G., 2015. Effects of landuse change on CH4 soil-atmospheric exchange in alpine meadow on the Tibetan Plateau. Pol. J. Environ. Stud. 24, 1593–1602.

Han, X., Domenech-Pascual, A., Casas-Ruiz, J., Donhauser, J., Jordaan, K., Ramond, J., Prieme, A., Romani, A., Frossard, A., 2024. Soil organic matter properties drive microbial enzyme activities and greenhouse gas fluxes along an elevational gradient. Geoderma 449, 116993.

He, G., Li, K., Liu, X., Gong, Y., Hu, Y., 2014. Fluxes of methane, carbon dioxide and nitrous oxide in an alpine wetland and an alpine grassland of the Tianshan Mountains, China. J. Arid. Land 6, 717–724.

Helbig, M., Chasmer, L.E., Kljun, N., Quinton, W.L., Treat, C.C., Sonnentag, O., 2017. The positive net radiative greenhouse gas forcing of increasing methane emissions from a thawing boreal forest-wetland landscape. Glob. Chang. Biol. 23, 2413–2427.

Hirota, M., Tang, Y., Hu, Q., Kato, T., Hirata, S., Mo, W., Cao, G., Mariko, S., 2005. The potential importance of grazing to the fluxes of carbon dioxide and methane in an alpine wetland on the Qinghai–Tibetan Plateau. Atmos. Environ. 39, 5255–5259.

Hofmann, K., Farbmacher, S., Illmer, P., 2016. Methane flux in montane and subalpine soils of the Central and Northern Alps. Geoderma 281, 83–89.

Hommeltenberg, J., Mauder, M., Drösler, M., Heidbach, K., Werle, P., Schmid, H.P., 2014. Ecosystem scale methane fluxes in a natural temperate bog–pine forest in southern Germany. Agric. For. Meteorol. 198–199, 273–284.

Hosono, T., Nouchi, I., 1997. Effect of gas pressure in the root and stem base zone on methane transport through rice bodies. Plant and Soil 195, 65–73.

Hugelius, G., Strauss, J., Zubrzycki, S., Harden, J., Schuur, E., Ping, C., Schirrmeister, L., Grosse, G., Michaelson, G., Koven, C., O'Donnell, J., Elberling, B., Mishra, U., Camill, P., Yu, Z., Palmtag, J., Kuhry, P., 2014. Estimated stocks of circumpolar permafrost carbon with quantified uncertainty ranges and identified data gaps. Biogeosciences 11, 6573–6593.

Hutchinson, G.L., Livingston, G.P., 1993. Use of chamber systems to measure trace gas fluxes. In Harper L, et al. (Eds.) Agricultural Ecosystem Effects on Trace Gases and Global Climate Change. ASA Special Publication 55, ASA, CSSA, SSSA, Madison, WI, pp. 63–78.

IPCC, 2021. In: Masson-Delmotte, V., Zhai, P., Pirani, A., Connors, S.L., Péan, C., Berger, S., Caud, N., Chen, Y., Goldfarb, L., Gomis, M.I., Huang, M., Leitzell, K., Lonnoy, E., Matthews, J.B.R., Maycock, T.K., Waterfield, T., Yelekçi, O., Yu, R., Zhou, B. (Eds.), Climate Change 2021: The Physical Science Basis. Contribution of Working Group I to the Sixth Assessment Report of the Intergovernmental Panel on Climate Change. Cambridge University Press, Cambridge, United Kingdom and New York, NY, USA.

Ishizuka, S., Sakata, T., Sawata, S., Ikeda, S., Sakai, H., Takenaka, C., Tamai, N., Onodera, S., Shimizu, T., Kan-na, K., Tanaka, N., Takahashi, M., 2009. Methane uptake rates in Japanese forest soils depend on the oxidation ability of topsoil, with a new estimate for global methane uptake in temperate forest. Biogeochemistry 92, 281–295.

Jackowicz-Korczyński, M., Christensen, T.R., Bäckstrand, K., Crill, P., Friborg, T., Mastepanov, M., Ström, L., 2010. Annual cycle of methane emission from a subarctic peatland. J. Geophys. Res. Biogeo. 115, G02009.

Jammet, M., Dengel, S., Kettner, E., Parmentier, F.J.W., Wik, M., Crill, P., Friborg, T., 2017. Year-round CH4 and CO2 flux dynamics in two contrasting freshwater ecosystems of the subarctic. Biogeosciences 14, 5189–5216.

Jiang, C., Yu, G., Fang, H., Cao, G., Li, Y., 2010. Short-term effect of increasing nitrogen deposition on CO2, CH4 and N2O fluxes in an alpine meadow on the Qinghai–Tibetan Plateau, China. Atmos. Environ. 44, 2920–2926.

Jiang, J., Yin, D., Sun, Z., Ye, B., Zhou, N., 2024. Global trend of methane abatement inventions and widening mismatch with methane emissions. Nat. Clim. Chang. 14, 393–401.

Juszczak, R., Augustin, J., 2013. Exchange of the greenhouse gases methane and nitrous oxide between the Aatmosphere and a temperate peatland in Central Europe. Wetlands 33, 895–907.

Kaiser, K., McGlynn, B., Dore, J., 2018. Landscape analysis of soil methane flux across complex terrain. Biogeosciences 15, 3143–3167.

Kang, H., Freeman, C., 2002. The influence of hydrochemistry on methane emissions from two contrasting northern wetlands. Water Air Soil Pollut. 141, 263–272.

Kato, T., Hirota, M., Tang, Y., Wada, E., 2011. Spatial variability of CH4 and N2O fluxes in alpine ecosystems on the Qinghai–Tibetan Plateau. Atmos. Environ. 45, 5632–5639.

Koyama, A., Johnson, N., Brewer, P., Webb, C., von Fischer, J., 2024. Biological and physical controls of methane uptake in grassland soils across the US Great Plains. Ecosphere 15, e4955.
Kwon, M.J., Beulig, F., Ilie, I., Wildner, M., Küsel, K., Merbold, L., Mahecha, M., Zimov, N., Zimov, S., Heimann, M., Schuur, E., Kostka, J., Kolle, O., Hilke, I., Göckede, M., 2017. Plants, microorganisms, and soil temperatures contribute to a decrease in methane fluxes on a drained Arctic floodplain. Glob. Chang. Biol. 23, 2396–2412.
Lee, J., Oh, Y., Lee, S., Seo, Y., Yun, J., Yang, Y., Kim, J., Zhuang, Q., Kang, H., 2023. Soil organic carbon is a key determinant of CH4 sink in global forest soils. Nat. Commun. 14, 3110.
Leppälä, M., Oksanen, J., Tuittila, E.S., 2011. Methane flux dynamics during mire succession. Oecologia 165, 489–499.
Li, T., Raivonen, M., Alekseychik, P., Aurela, M., Lohila, A., Zheng, X., Zhang, Q., Wang, G., Mammarella, I., Rinne, J., Yu, L., Xie, B., Vesala, T., Zhang, W., 2016. Importance of vegetation classes in modeling CH4 emissions from boreal and subarctic wetlands in Finland. Sci. Total Environ. 572, 1111–1122.
Li, Y., Dong, S., Liu, S., Zhou, H., Gao, Q., Cao, G., Wang, X., Su, X., Zhang, Y., Tang, L., Zhao, H., Wu, X., 2015. Seasonal changes of CO2, CH4 and N2O fluxes in different types of alpine grassland in the Qinghai–Tibetan Plateau of China. Soil Biol. Biochem. 80, 306–314.
Liu, S., Zamanian, K., Schleuss, P., Zarebanadkouki, M., Kuzyakov, Y., 2018. Degradation of Tibetan grasslands: consequences for carbon and nutrient cycles. Agric. Ecosyst. Environ. 252, 93–104.
Luo, G., Kiese, R., Wolf, B., Butterbach-Bahl, K., 2013. Effects of soil temperature and moisture on methane uptake and nitrous oxide emissions across three different ecosystem types. Biogeosciences 10, 3205–3219.
Mast, M., Wickland, K., Striegl, R., Clow, D., 1998. Winter fluxes of CO2 and CH4 from subalpine soils in Rocky Mountain National Park, Colorado. Global Biogeochem. Cycles 12, 607–620.
Mastepanov, M., Sigsgaard, C., Dlugokencky, E.J., Houweling, S., Ström, L., Tamstorf, M. P., Christensen, T.R., 2008. Large tundra methane burst during onset of freezing. Nature 456, 628.
Mosier, A.R., Parton, W.J., Valentine, D.W., Ojima, D.S., Schimel, D.S., Delgado, J.A., 1996. CH4 and N2O fluxes in the Colorado shortgrass steppe: 1. Impact of landscape and nitrogen addition. Global Biogeochem. Cycles 10, 387–399.
Nilsson, M., Sagerfors, J., Buffam, I., Laudon, H., Eriksson, T., Grelle, A., Klemedtsson, L., Weslien, P., Lindroth, A., 2008. Contemporary carbon accumulation in a boreal oligotrophic minerogenic mire–a significant sink after accounting for all C-fluxes. Glob. Chang. Biol. 14, 2317–2332.
Nisbet, E., 2023. New hope for methane reduction. Science 382, 1093.
Olefeldt, D., Turetsky, M., Crill, P., Mcguire, A., 2013. Environmental and physical controls on northern terrestrial methane emissions across permafrost zones. Glob. Chang. Biol. 19, 589–603.
Olson, D.M., Griffis, T.J., Noormets, A., Kolka, R., Chen, J., 2013. Interannual, seasonal, and retrospective analysis of the methane and carbon dioxide budgets of a temperate peatland. J. Geophys. Res. Biogeosci. 118, 226–238.
Peng, H., Guo, Q., Ding, H., Hong, B., Zhu, Y., Hong, Y., Cai, C., Wang, Y., Yuan, L., 2019. Multi-scale temporal variation in methane emission from an alpine peatland on the eastern Qinghai-Tibetan Plateau and associated environment. Agric. For. Meteorol. 276–277, 107616.
Plain, C., Ndiaye, F., Bonnaud, P., Ranger, J., Epron, D., 2019. Impact of vegetation on the methane budget of a temperate forest. New Phytol. 221, 1447–1456.
Potter, C., Davidson, E., Verchot, L., 1996. Estimation of global biogeochemical controls and seasonality in soil methane consumption. Chemosphere 32, 2219–2246.
Reay, D., Radajewski, S., Murrell, J., McNamara, N., Nedwell, D., 2001. Effects of land-use on the activity and diversity of methane oxidizing bacteria in forest soils. Soil Biol. Biochem. 33, 1613–1623.
Rinne, J., Riutta, T., Pihlatie, M., Aurela, M., Haapanala, S., Tuovinen, J.P., Tuittila, E.S., Vesala, T., 2007. Annual cycle of methane emission from a boreal fen measured by the eddy covariance technique. Tellus B 59, 449–457.
Riveros-Iregui, D., McGlynn, B., 2009. Landscape structure control on soil CO2 efflux variability in complex terrain: Scaling from point observations to watershed scale fluxes. J. Geophys. Res. Biogeosci. 114, G02010.
Rong, Y., Ma, L., Johnson, D.A., 2015. Methane uptake by four land-use types in the agro-pastoral region of northern China. Atmos. Environ. 116, 12–21.
Saunosi, M., Stavert, A., Poulter, B., Bousquet, P., Canadell, J., Jackson, R., et al., 2020. The global methane budget 2000-2017. Earth Syst. Sci. Data 12, 1561–1623.
Shindell, D., Kuylenstierna, J., Vignati, E., Dingenen, R., Amann, M., Klimont, Z., Anenberg, S., Muller, N., Janssensmaenhout, G., Raes, F., Schwartz, J., Faluvegi, G., Pozzoli, L., Kupiainen, K., Holglund-Isaksson, L., Emberson, L., Streets, D., Ramanathan, V., Hicks, K., Oanh, N., Milly, G., Williams, M., Demkine, V., Fowler, D., 2012. Simultaneously mitigating near-term climate change and improving human health and food security. Science 335, 183–189.
Smith, K., Ball, T., Conen, F., Dobbie, K., Massheder, J., Rey, A., 2003. Exchange of greenhouse gases between soil and atmosphere: interactions of soil physical factors and biological processes. Eur. J. Soil Sci. 54, 779–791.
Sommerfeld, R., Mosier, A., Musselman, R., 1993. CO2, CH4 and N2O flux through a Wyoming snowpack and implications for global budgets. Nature 361, 140–142.
Song, C., Xu, X., Sun, X., Tian, H., Sun, L., Miao, Y., Wang, X., Guo, Y., 2012. Large methane emission upon spring thaw from natural wetlands in the northern permafrost region. Environ. Res. Lett. 7, 034009.
Song, C.C., Xu, X.F., Tian, H.Q., Wang, Y.Y., 2009. Ecosystem–atmosphere exchange of CH4 and N2O and ecosystem respiration in wetlands in the Sanjiang Plain, Northeastern China. Glob. Chang. Biol. 15, 692–705.
Song, W.M., Wang, H., Wang, G., Chen, L., Jin, Z., Zhuang, Q., He, J., 2015. Methane emissions from an alpine wetland on the Tibetan Plateau: Neglected but vital contribution of the nongrowing season. J. Geophys. Res. Biogeo. 120, 1475–1490.
Steinkamp, R., Butterbach-Bahl, K., Papen, H., 2001. Methane oxidation by soils of a N-limited and N-fertilized spruce forest in the Black Forest, Germany. Soil Biol. Biochem. 33, 145–153.
Tate, K., Ross, D., Saggar, S., Hedley, C., Dando, J., Singh, B., Lambie, S., 2007. Methane uptake in soils from pinus radiata plantations, a reverting shrubland and adjacent pastures: effects of land-use change, and soil texture, water and mineral nitrogen. Soil Biol. Biochem. 39, 1437–1449.
Terrer, C., Vicca, S., Hungate, B., Phillips, R., Prentice, I., 2016. Mycorrhizal association as a primary control of the CO2 fertilization effect. Science 353, 72–74.
Treat, C.C., Bloom, A.A., Marushchak, M.E., 2018. Nongrowing season methane emissions–a significant component of annual emissions across northern ecosystems. Glob. Chang. Biol. 24, 3331–3343.
Turetsky, M.R., Kotowska, A., Bubier, J., Dise, N.B., Crill, P., Hornibrook, E.R., Minkkinen, K., Moore, T., Myers-Smith, I., Nykänen, H., Olefeldt, D., Rinne, J., Saarnio, S., Shurpali, N., Tuittila, E., Waddington, J., White, J., Wickland, K., Wilmking, M., 2014. A synthesis of methane emissions from 71 northern, temperate, and subtropical wetlands. Glob. Chang. Biol. 20, 2183–2197.
Ueyama, M., Takeuchi, R., Takahashi, Y., Ide, R., Ataka, M., Kosugi, Y., Takahashi, K., Saigusa, N., 2015. Methane uptake in a temperate forest soil using continuous closed–chamber measurements. Agric. For. Meteorol. 213, 1–9.
Wang, Y., Xiao, J., Ma, Y., Ding, J., Chen, X., Ding, Z., Luo, Y., 2023. Persistent and enhanced carbon sequestration capacity of alpine grasslands on Earth's Third Pole. Sci. Adv. 9, eade6875.
Wangari, E., Mwanake, R., Houska, T., Kraus, D., Gettel, G., Kiese, R., Breuer, L., Butterbach-Bahl, K., 2023. Identifying landscape hot and cold spots of soil greenhouse gas fluxes by combining field measurements and remote sensing data. Biogeosciences 20, 5029–5067.
Wei, D., Xu, R., Tenzin-Tarchen, Wang, Y., Wang, Y., 2015. Considerable methane uptake by alpine grasslands despite the cold climate: in situ measurements on the central Tibetan Plateau, 2008–2013. Glob. Chang. Biol. 21, 777–788.
West, A., Brooks, P., Fisk, M., Smith, L., Holland, E., Jaeger, C., Babcock, S., Lai, R., Schmidt, S., 1999. Landscape patterns of CH4 fluxes in an alpine tundra ecosystem. Biogeochemistry 45, 243–264.
Whalen, S.C., Reeburgh, W.S., 1992. Interannual variations in tundra methane emission: a 4-year time series at fixed sites. Global Biogeochem. Cycles 6, 139–159.
Wille, C., Kutzbach, L., Sachs, T., Wagner, D., Pfeiffer, E.M., 2008. Methane emission from Siberian arctic polygonal tundra: eddy covariance measurements and modeling. Glob. Chang. Biol. 14, 1395–1408.
Wilson, D., Farrell, C.A., Fallon, D., Moser, G., Muller, C., Renou-wilson, F., 2016. Multiyear greenhouse gas balances at a rewetted temperate peatland. Glob. Chang. Biol. 22, 4080–4095.
WMO, 2019. The State of Greenhouse Gases in the Atmosphere Based on Global Observations Through 2018, 15. WMO Greenhouse Gas Bulletin, pp. 1–8.
Wu, X., Yao, Z., Brüggemann, N., Shen, Z., Wolf, B., Dannenmann, M., Zheng, X., Butterbach-Bahl, K., 2010. Effects of soil moisture and temperature on CO2 and CH4 soil-atmosphere exchange of various land use/cover types in a semi-arid grassland in Inner Mongolia, China. Soil Biol. Biochem. 42, 773–787.
Xiang, S.A., Guo, R.Q., Wu, N., Sun, S.C., 2009. Current status and future prospects of Zoige Marsh in Eastern Qinghai–Tibet Plateau. Ecol. Eng. 35, 553–562.
Yang, G., Zheng, Z., Abbott, B., Olefeldt, D., Knoblauch, C., Song, Y., Kang, L., Qin, S., Peng, Y., Yang, Y., 2023. Characteristics of methane emissions from alpine thermokarst lakes on the Tibetan Plateau. Nat. Commun. 14, 3121.
Yao, Z., Wang, R., Zhang, H., Ma, L., Zheng, X., Liu, C., Zhang, W., Wang, Y., Zhu, B., Butterbach-Bahl, K., 2025. Rodent-induced grassland degradation increases annual non-CO2 greenhouse gas fluxes and NO losses despite CH4 uptake enhancement. Agric. For. Meteorol. 368, 110534.
Yao, Z., Wang, Y., Wang, R., Wang, X., Wang, Y., Zheng, X., Liu, C., Zhu, B., Zhou, M., Liu, Y., Butterbach-Bahl, K., 2024. Long-term straw return to a wheat-maize system results in topsoil organic C saturation and increased yields while no stimulating or reducing yield-scaled N2O and NO emissions. Agric. For. Meteorol. 349, 109937.
Yao, Z., Wu, X., Wolf, B., Dannenmann, M., Butterbach-Bahl, K., Brüggemann, N., Chen, W., Zheng, X., 2010. Soil-atmosphere exchange potential of NO and N2O in different land use types of Inner Mongolia as affected by soil temperature, soil moisture, freeze-thaw, and drying-wetting events. J. Geophys. Res. Atmos. 115, D17116.
Yao, Z., Yan, G., Ma, L., Wang, Y., Zhang, H., Zheng, X., Wang, R., Liu, C., Wang, Y., Zhu, B., Zhou, M., Rahimi, J., Butterbach-Bahl, K., 2022. Soil C/N ratio is the dominant control of annual N2O fluxes from organic soils of natural and semi-natural ecosystems. Agric. For. Meteorol. 327, 109198.
Yu, L., Huang, Y., Zhang, W., Li, T., Sun, W., 2017. Methane uptake in global forest and grassland soils from 1981 to 2010. Sci. Total Environ. 607–608, 1163–1172.
Yu, L., Wang, H., Wang, G., Song, W., Huang, Y., Li, S., Liang, N., Tang, Y., He, J., 2013. A comparison of methane emission measurements using Eddy Covariance and manual and automated chamber–based techniques in Tibetan Plateau alpine wetland. Environ. Pollut. 181, 81–90.
Yu, L., Zhu, J., Zhang, X., Wang, Z., Dörsch, P., Mulder, J., 2019. Humid subtropical forests constitute a net methane source: a catchment-scale study. J. Geophys. Res. Biogeo. 124, 2927–2942.
Zhang, H., Yao, Z., Ma, L., Zheng, X., Wang, R., Wang, K., Liu, C., Zhang, W., Zhu, B., Tang, X., Hu, Z., Han, S., 2019. Annual methane emissions from degraded alpine wetlands in the eastern Tibetan Plateau. Sci. Total Environ. 657, 1323–1333.
Zhang, L., Zhang, S., Xia, X., Battin, T., Liu, S., Wang, Q., Liu, R., Yang, Z., Ni, J., Stanley, E., 2022. Unexpectedly minor nitrous oxide emissions from fluvial networks

draining permafrost catchments of the east Qinghai-Tibet Plateau. Nat. Commun. 13, 950.
Zhao, B., Zhuang, Q., 2024. Nitrogen cycling feedback on carbon dynamics leads to greater CH4 emissions and weaker cooling effect of northern peatlands. Global Biogeochem. Cycles 38, e2023GB007978.
Zhou, X., Xiao, W., Cheng, L., Smaill, S., Peng, S., 2024. Unveiling the impact of soil methane sink on atmospheric methane concentrations in 2020. Glob. Chang. Biol. 30, e17381.
Zhu, X., Luo, C., Wang, S., Zhang, Z., Cui, S., Bao, X., Jiang, L., Li, Y., Li, X., Wang, Q., Zhou, Y., 2015. Effects of warming, grazing/cutting and nitrogen fertilization on greenhouse gas fluxes during growing seasons in an alpine meadow on the Tibetan Plateau. Agric. For. Meteorol. 214–215, 506–514.
Zona, D., Gioli, B., Commane, R., Lindaas, J., Wofsy, S.C., Miller, C.E., Dinardo, S.J., Dengel, S., Sweeney, C., Karion, A., Chang, R.Y.W., Henderson, J.M., Murphy, P.C., Goodrich, J.P., Moreaux, V., Liljedahl, A., Watts, J.D., Kimball, J.S., Lipson, D.A., Oechel, W.C., 2016. Cold season emissions dominate the Arctic tundra methane budget. PNAS 113, 40–45.